Modelling organic aerosol over Europe in summer conditions with the VBS-GECKO parameterization: sensitivity to secondary organic compound properties and IVOC emissions

Victor Lannuque[1,2,3,a], Florian Couvidat[2], Marie Camredon[1], Bernard Aumont[1] and Bertrand Bessagnet[2,b]

[1] LISA, UMR CNRS 7583, IPSL, Université Paris Est Créteil and Université Paris Diderot, 94010 Créteil Cedex, France.
[2] INERIS, National Institute for Industrial Environment and Risks, Parc Technologique ALATA, 60550 Verneuil-en-Halatte, France.
[3] Agence de l'Environnement et de la Maîtrise de l'Energie, 20 avenue du Grésillé - BP 90406, 49004 Angers Cedex 01, France.
[a] Now at: Laboratoire d'Aérologie, Université de Toulouse, CNRS, UPS, Toulouse, France.
[b] Now at: Hangzhou Futuris Environmental Technology Co. Ltd, Zhejiang Overseas High-Level Talent Innovation Park, No. 998 WenYi Road, 311121, Hangzhou, Zhejiang, China.

Correspondence to: Victor Lannuque (victor.lannuque@gmail.com) and Florian Couvidat (florian.couvidat@ineris.fr)

Abstract. The VBS-GECKO parameterization for secondary organic aerosol (SOA) formation was integrated in the chemistry-transport model CHIMERE. Concentrations of organic aerosol (OA) and SOA were simulated over Europe for the July-August 2013 period. Simulated concentrations with the VBS-GECKO were compared to results obtained with the former H^2O parameterization implemented in CHIMERE and to observations from EMEP, ACTRIS and other observations available in the EBAS database. The model configuration using the VBS-GECKO parameterization slightly improves the performances compared to the model configuration using the former H^2O parameterisation. The VBS-GECKO model configuration performs well for stations showing a large SOA concentration from biogenic sources, especially in northern Europe but underestimate OA concentrations over stations close to urban areas. Simulated OA was found to be mainly secondary (~85%) and from terpene oxidation. Simulations show negligible contribution of the oxidation of mono-aromatic compounds to SOA production. Tests performed to examine the sensitivity of simulated OA concentrations to hydro-solubility, volatility, ageing rates and NO_x regime have shown that the VBS-GECKO parameterization provides consistent results, with a weak sensitivity to changes in the parameters provided by the gas phase mechanism included in CHIMERE (e.g. HO_x or NO_x concentrations). Different emission scenarios (from heavy diesel to light gasoline fleet) were tested to examine the contribution of S/IVOC oxidation to SOA production. At the continental scale, these simulations show a weak sensitivity of OA concentrations to the vehicle fleet. At the local scale, accounting for IVOC emission was found to lead to a substantial increase of OA concentrations in the plume from urban areas, especially if diesel fleet case is assumed. This additional OA source remains too small to explain the gap between simulated and measured values at stations where anthropogenic sources are dominant.

1. Introduction

For the past 20 years, fine particulate matter or $PM_{2.5}$ (particles with a diameter smaller than 2.5 µm) has been regulated due to their health impacts and the resulting costs (e.g. Lim et al., 2012; WHO Regional Office for Europe and OECD, 2015).

5   Furthermore, fine particles degrade visibility (e.g. Han et al., 2012) and influence climate change (e.g. Boucher et al., 2013). Organic aerosol (OA) represents a large fraction of the total fine particle mass (e.g. Jimenez et al., 2009). This OA is either primary (directly emitted into the atmosphere) or secondary (formed by gas/particle partitioning of low volatile and/or highly soluble species produced during the oxidation of gaseous organic compounds) (e.g. Carlton et al., 2009; Kroll and Seinfeld, 2008). The secondary organic aerosol (SOA) dominates the primary organic aerosol (POA) in most environments (e.g.

10 Gelencsér et al., 2007; Jimenez et al., 2009).

Chemistry-transport models (CTMs) are used to investigate and identify air quality regulation policies, but fall short to reproduce the secondary fraction of the OA (Bessagnet et al., 2016; Solazzo et al., 2012; Tsigaridis et al., 2014). These difficulties are due to (i) the complexity of the processes leading to SOA formation (gas and particle phase chemistry, non-ideal behaviour, gas/particle mass transfer limitation, etc.) and (ii) the large number and the diversity of organic species

15 contributing to SOA composition.

Several parameterisations have been developed and used in CTM to represent SOA formation. Until 2006, two main approaches were followed to describe SOA formation: the two-product model and the molecular approach. The two-product model (Odum et al., 1996; Schell et al., 2001), based on experimental SOA yields measured in atmospheric chambers, represents SOA formation from the condensation onto particles of semi-volatile organic compounds formed after one

20 gaseous oxidation step of an emitted volatile organic precursor. In the molecular approach (Pun et al., 2002, 2003), semi-volatile and/or hydro-soluble compounds are lumped by molecular structures and experimental physico-chemical properties are associated to each surrogate species to estimate their phase partitioning. Comparisons with field observations have shown that CTMs using these former parameterizations under-estimated SOA mass concentrations (e.g. Heald et al., 2005; Pun et al., 2006a;Volkamer et al., 2006). Additional processes were then included in the parameterizations to improve the

25 simulations of SOA concentrations, such as gas phase ageing, multiphase chemistry and more comprehensive emissions. Robinson et al. (2007) have indeed showed that POA provided in emission inventories are semi-volatile organic compounds (SVOC) (existing both in particle and gas phases) and that a fraction of emitted organic compounds are intermediate-volatility organic compounds (IVOC) (forming SOA after several oxidation stages) (e.g. Ots et al., 2016; Robinson et al., 2007; Woody et al., 2015). The Volatility Basis Set (VBS) approach (Donahue et al., 2006, 2012) has been the first SOA

30 parameterization to include IVOC and SVOC emissions, representing SOA formation by the evolution of a discretized distribution of S/IVOC into volatility bins. The VBS is the first approach considering the ageing of SOA (i.e. evolution of SOA after formation, e.g. Rudich et al., 2007) by gaseous oxidation of the semi-volatile organic compounds.

Other studies have highlighted the important role played by condensed phase processes in SOA formation, in particular the reactivity of hydrophilic products in the aqueous phase (e.g. Couvidat et al., 2012; Couvidat and Seigneur, 2011; Knote et al., 2014; Paulot et al., 2009; Pun et al., 2006b; Surratt et al., 2010), the oligomerization of SVOC in both organic and aqueous phase (e.g. Aksoyoglu et al., 2011; Couvidat et al., 2012; Denkenberger et al., 2007; Dommen et al., 2006; Kalberer et al., 2006; Lemaire et al., 2016; Trump and Donahue, 2014), the non-ideal behaviour of the organic aerosol (Couvidat et al., 2012, Couvidat and Sartelet, 2015; Pun et al., 2006; Pye et al., 2018) or the effect of the aerosol viscosity (Couvidat and Sartelet, 2015; Shiraiwa et al., 2013). However, most CTMs still fall short to reproduce SOA concentration with up to date parameterizations (e.g. Aksoyoglu et al., 2011; Bessagnet et al., 2016; Ciarelli et al., 2016; Couvidat et al., 2012; Im et al., 2015; Petetin et al., 2014; Solazzo et al., 2012). These SOA parameterizations are optimized/built on the basis of atmospheric chamber data. Experiments are however limited in number and are usually performed under conditions that differ from the atmosphere. In addition, SOA formation experiments can be subject to potential artefacts from chamber wall surfaces, such as aerosol and gaseous compound wall losses (e.g. La et al., 2016; Matsunaga and Ziemann, 2010; McMurry and Grosjean, 1985). Considering or not these artefacts for the parameterization development directly impact SOA representation in air quality models (Cappa et al. 2016).

The development of the VBS-GECKO parameterization explores another track using the results of an explicit model representing the state of knowledge of organic gas-phase chemistry instead of atmospheric chamber data. The VBS-GECKO parameterization for SOA formation (Lannuque et al., 2018) is a VBS-type parameterization with ageing. VBS-GECKO was optimized based on box modelling results using explicit oxidation mechanisms generated with the Generator for Explicit Chemistry and Kinetics of Organics in the Atmosphere (GECKO-A) modelling tool (Aumont et al, 2005; Camredon et al, 2007).

The objectives of this study are (i) to evaluate the behaviour of the VBS-GECKO parameterization in the CTM CHIMERE (Menut et al., 2013, Mailler et al., 2017) by comparison with field measurements and previous simulations obtained with the H^2O parameterization (Couvidat et al., 2012) already implemented in CHIMERE, (ii) to explore the sensitivity of simulated SOA concentration to organic compound properties (volatility, solubility, ageing rates or NO_x regime) and (iii) to test different representations of S/IVOC emissions from traffic, especially considering various car fleet (with different diesel/gasoline ratio). The CHIMERE model setup and the VBS-GECKO implementations are described in section 2. In section 3, the VBS-GECKO is evaluated over Europe for a two-month summer period, the sensitivity to several key parameters is explored in section 4. Different scenarios for S/IVOC emissions are investigated in section 5 and, finally, results on simulated OA sources and concentrations are discussed in section 6.

2. Method

2.1. The CHIMERE chemical transport model

The evaluation of the VBS-GECKO parameterization and the exploration of SOA sensitivity were performed using the CHIMERE 2017 β version. This version is based on the CHIMERE 2013 version (Menut et al., 2013) which was modified to

5　implement a new aerosol module and improve the representation of particles. Details of the CHIMERE 2017 β version and its evaluation are given in Couvidat et al. (2018).

Briefly, the CHIMERE 2017 β version uses the MELCHIOR2 gas-phase chemical scheme, involving 44 species reacting according to 120 reactions. MELCHIOR2 is a reduced version of the MELCHIOR1 mechanism, obtained by the Carter's surrogate molecule method (Carter, 1990). In CHIMERE, the aerosol evolution is described by a sectional aerosol module

10　(e.g. Bessagnet et al., 2004, 2009; Schmidt et al., 2001). The size distribution of aerosol particles is here represented using 9 bins, ranging from 10 nm to 10 μm. Aerosol formation is represented in the model by nucleation for sulfuric acid (Kulmala et al., 1998), coagulation between particles (e.g. Debry et al., 2007; Jacobson et al., 1994) and condensation/evaporation via absorption according to the "bulk equilibrium" approach (e.g. Pandis et al., 1993). For inorganic species, the gas/particle equilibrium concentrations are calculated using the ISORROPIA v2.1 (Fountoukis and Nenes, 2007) thermodynamic

15　module. For organic species, the equilibrium concentrations are calculated using the SOAP (Secondary Organic Aerosol Processor) thermodynamic module (Couvidat and Sartelet, 2015). The gaseous formation of secondary organic species able to partition between the gas and the condensed phases (so leading to SOA formation) are represented in the CHIMERE β version using the H^2O mechanism. Here, the VBS-GECKO parameterization has also been implemented. The H^2O and VBS-GECKO organic aerosol modules are described hereafter.

20　The chemical speciation of emitted non-methane volatile organic compounds (NMVOC) is taken from Passant (2002) as described in Menut et al. (2013). Primary organic aerosol (POA) from emission inventories are considered as SVOC. A SVOC/POA ratio of 1 is used for all the activity sectors except for residential emissions where a SVOC/POA ratio of 5 is used assuming that wood burning emissions are underestimated (e.g. Denier Van Der Gon et al., 2015). This factor was shown to give satisfactory results (Couvidat et al. 2012, 2018). Biogenic emissions are computed with the Model of

25　Emissions and Gases and Aerosols from Nature MEGAN 2.1 algorithm (Guenther et al., 2012). Dry deposition for gaseous organic species is described using the Wesely (1989) parameterization and according to their Henry's law constants, as described by Bessagnet et al. (2010).

2.2. The organic aerosol modules

2.2.1. The H^2O reference mechanism

30　The H^2O mechanism (Couvidat et al., 2018) considers SOA formation from the partitioning of hydrophilic species (condensing mainly on an aqueous phase) and hydrophobic species (condensing only on an organic phase owing to their low affinity with water). Hydrophilic species may also condense on an organic phase in the absence of aqueous particles, i.e. at

very low relative humidity. Distinction between hydrophobic and hydrophilic compounds is based on their octanol/water coefficient (Pun et al., 2006) or their partitioning between the organic and aqueous phases (Couvidat and Seigneur, 2011). H^2O considers the formation of hydrophilic and/or hydrophobic species from the gaseous oxidation of isoprene, monoterpenes (α-pinene, β-pinene, limonene and ocimene), sesquiterpenes (humulene) and mono-aromatic precursors

5   (toluene and xylenes). Note that in H^2O, limonene mechanism is used as a surrogate mechanism for ocimene (ocimene having its own OH, NO_3 and O_3 reaction rates). Each emitted SOA precursor is linked to a species of the H^2O mechanism. POA provided by emissions inventories are split into three emitted compounds having a "low", "medium" and "high" volatility with a fraction that follows the POA volatility distribution given in Robinson et al. (2007). The aging of these three compounds with OH leads to hydrophobic species with a lower volatility. No gaseous oxidation is considered for these

10   hydrophylic and hydrophobic species in H^2O. H^2O has been evaluated over Europe (Couvidat et al., 2012, 2018) and the Paris area (Couvidat et al., 2013; Zhu et al., 2016a, 2016b). The H^2O reference mechanism is presented in table S1 of supplementary material.

2.2.2.   The VBS-GECKO parameterization

The VBS-GECKO parameterization (Lannuque et al., 2018) represents SOA formation from the partitioning of low volatile

15   organic compounds onto an organic aerosol phase. This is a Volatility Basis Set (VBS) type parameterization optimized on explicit simulations of gas phase oxidation and SOA formation. VBS-GECKO considers the formation of 7 volatility bins, and includes bin ageing with OH and photolysis, for the oxidation of monoterpenes (α-pinene, β-pinene and limonene), mono-aromatic compounds (benzene, toluene, and o- m- and p-xylenes), n-alkanes (decane, tetradecane, octadecane, docosane and hexacosane) and linear 1-alkenes (decene, tetradecene, octadecene, docosene and hexacosene). Although

20   considered as distinct species, the 7 volatility bins produced from each precursor have identical properties. The volatility bins are simply named VB(1-7) hereafter except if information regarding the parent hydrocarbon is required. Table 1 gives the molar weights (Mw), saturation vapour pressures (P^{sat}) at 298 K, effective Henry's law constants (H^{eff}) at 298K and vaporizations enthalpies (ΔH_{vap}) used for the VBS-GECKO species. For the comparisons with in-situ measurements, the OM:OC ratio of the volatility bins are assumed to be equal to 1.8, in agreement with typical observed values given by

25   Canagaratna et al. (2015).

For each parent compound, the production and aging of the 7 volatility bins depend on NO_x regime. The stoichiometric coefficients depend on the reaction rate ratio (RRR) of RO_2 with NO and have been optimized for 5 RRR values: 0, 0.1, 0.5, 0.9 and 1 (Lannuque et al., 2018). The entire RRR range is covered by linear interpolation. In CHIMERE, RRR is calculated in each box at each chemical time step.

30   The former H^2O parameterization in CHIMERE was replaced by the VBS-GECKO parameterization for SOA production from terpenes and mono-aromatic compounds. The VBS-GECKO mechanisms were also implemented in CHIMERE for SOA formation from low volatile NMVOC (i.e. alkanes and alkenes from C10 to C13), gaseous species usually not considered in 3D models as SOA precursors. Each emitted SOA precursor not present in the VBS-GECKO was linked to a

VBS-GECKO species. As in the H^2O mechanism, the VBS-GECKO parameterization for limonene was used as a surrogate mechanism for ocimene. The VBS-GECKO parameterizations for benzene, toluene, o-, m- and p-xylenes were also used as surrogate mechanisms for other emitted mono-aromatic compounds according to their SOA yield and reactivity with OH. n-dodecane and tetradecane VBS-GECKO species were used to lump emitted alkanes with 10 to 13 atoms of carbon,

5   according to their carbon chain length. The VBS-GECKO mechanism for 1-decene was applied for all emitted C10 alkenes. The lumping scheme between emitted NMVOC and VBS-GECKO species is given in Table 2. The current VBS-GECKO version does not represent SOA production from the oxidation of isoprene and sesquiterpenes. The H^2O parameterizations for isoprene and humulene were therefore left unchanged in CHIMERE to account for this SOA production. The H^2O parameterization was as a first step also used to account for SOA formation from primary SVOC. This implementation of the

10   VBS-GECKO in CHIMERE was selected here as the reference configuration and is denoted ref-VBS-GECKO hereafter. The ref-VBS-GECKO mechanism is presented in table S2 of supplementary material and evaluated in section 3. Changes were then applied to this configuration to perform sensitivity tests of SOA formation on secondary organic compound properties (section 4), and on S/IVOC emissions (section 5).

2.3.   Simulation setup and field measurements

15   The model was run to simulate the concentrations of OA over Europe (from 25° W to 45° E in longitude and from 30° to 70° N in latitude) with an horizontal resolution of 0.25° × 0.25° during the July-August 2013 period, SOA formation being expected to be important during summertime. Meteorology was obtained from Integrated Forecasting System (IFS) model of the European Centre for Medium-Range Weather Forecasts (ECMWF). This meteorology has been evaluated in Bessagnet et al. (2016) for the model intercomparison project EURODELTA-III. ECMWF in the EURODELTA-III project was shown to

20   be one of the most representative models over Europe. Anthropogenic emissions of gases and particles were taken from the European Monitoring and Evaluation Programme (EMEP) inventory (methodology described in Vestreng, 2003) and boundary conditions were generated from the Model for OZone And Related Tracers (Mozart v4.0 (Emmons et al., 2010)). Wildfire emissions were not considered.

The VBS-GECKO mechanism was evaluated comparing the simulated results to the H^2O mechanism and particulate phase

25   measurements available in the EBAS database (http://ebas.nilu.no/). EBAS is a database hosting observation data of atmospheric chemical composition and physical properties in support of a number of national and international programs ranging from monitoring activities to research projects. EBAS is developed and operated by the Norwegian Institute for Air Research (NILU). This database is populated for example by the EMEP measurements (Tørseth et al., 2012) or the Aerosols, Clouds and Trace gases Research Infrastructure (ACTRIS, http://www.actris.eu/) ones. 48 rural background stations provide

30   measurements for fine particulate matter and were thus selected here for a statistical evaluation: 36 stations for $PM_{2.5}$, 13 for $OC_{PM2.5}$ (organic carbon in $PM_{2.5}$) and 6 for OM_{PM1} (organic matter in PM_1). The location of the selected stations is shown in Fig. 1.a. Among these stations, 7 stations were used for time series comparisons:

Atmospheric
Chemistry
and Physics
Discussions

- the NL0644R (Cabauw, Netherlands), DE0044R (Melpitz, Germany) and FR0020R (SIRTA, Palaiseau, France) rural background stations, located in areas dominantly impacted by anthropogenic air masses (see Figure S1 in supplementary material presenting the mean of the simulated ratios between toluene and α-pinene emission fluxes for the studied period).

- the NO0002R (Birkenes II, Norway), PL0005R (Diabla Gora, Poland), FI0050R (Hyytiälä, Finland) and SI0008R (Iskrba, Slovenia) rural background stations, located in areas dominantly impacted by biogenic emissions (see Figure S1 in supplementary material).

The location of these 7 stations is shown in Fig. 1.b.

Various statistical indicators were computed to evaluate the VBS-GECKO mechanism, including the Root Mean Square Error (RMSE), the correlation coefficient, the Mean Fractional Error (MFE) and the Mean Fractional Bias (MFB). MFB and MFE are calculated as:

$$MFB = \frac{1}{N}\sum_{i=1}^{N} \frac{\left(c_i^{mod} - c_i^{obs}\right)}{\left(\frac{c_i^{mod} + c_i^{obs}}{2}\right)},$$ (1)

$$MFE = \frac{1}{N}\sum_{i=1}^{N} \frac{\left|c_i^{mod} - c_i^{obs}\right|}{\left(\frac{c_i^{mod} + c_i^{obs}}{2}\right)},$$ (2)

where c_i^{mod} and c_i^{obs} are the simulated and observed concentrations of the studied component at the time i. and N the number of available in-situ measurement values. Boylan and Russell (2006) defined two criteria to estimate the performances of a model. The model performance criteria (described as the level of accuracy that is considered to be acceptable for modelling applications) is reached when MFE ≤ 75% and |MFB| ≤ 50% whereas the performance goal (described as the level of accuracy that is considered to be close to the best values a model can be expected to achieve) is reached when MFE ≤ 50% and |MFB| ≤ 30%. Although these criteria are not recent, they provide a useful basis to evaluate the reliability of the models.

3. Evaluation of the ref-VBS-GECKO parameterization

Figure 2.a shows the mean OA mass concentrations simulated with the ref-VBS-GECKO version for the July-August 2013 period. The simulated mean OA concentrations range from ~0 μg.m^{-3} in remote oceanic areas, to ~12 μg m^{-3} around the Adriatic Sea and in the northern Italy, and are coherent with the expected orders of magnitude and spatial distribution over Europe (Aksoyoglu et al., 2011; Crippa et al, 2014). Figure 2.b presents the relative difference between mean OA mass concentrations simulated with ref-VBS-GECKO and with H^{2}O. The ref-VBS-GECKO produces more OA than H^{2}O, with a mean OA mass concentration around 30% higher on average over Europe. The increase is particularly important over northern Europe, with maximum differences reaching around +60%.

Table 3 gathers the statistical results calculated on daily averaged concentrations for ref-VBS-GECKO at the 48 stations (RMSE, R, MFB and MFE), as well as the difference of this statistical indicator between ref-VBS-GECKO and H^{2}O. Globally, statistical indicators show a high spatiotemporal correlation between ref-VBS-GECKO and measurements for daily OM$_{PM1}$ and OC$_{PM2.5}$ with R > 0.5 (0.79 and 0.57 respectively). For daily averaged measurements of PM$_{2.5}$, the correlation is

smaller (0.42). This lower correlation for $PM_{2.5}$ has already been highlighted in summertime during the EURODELTA-III inter-comparison campaign (Bessagnet et al., 2016). MFE and MFB satisfy the performance criteria of Boylan and Russel (2006) for all the measurements. However, daily averaged $PM_{2.5}$, and especially the organic fraction (OM_{PM1} and $OC_{PM2.5}$), appear to be systematically underestimated by the ref-VBS-GECKO model.

5　Comparing ref-VBS-GECKO statistical results with H^2O statistical results, the simulated daily averaged $PM_{2.5}$ concentrations over the 36 stations appear to be weakly sensitive to the SOA formation mechanism used in the model. Only a slight improvement due to an increase in simulated $PM_{2.5}$ concentrations of about 5.5% is observed with the ref-VBS-GECKO model configuration. Concerning simulated $OC_{PM2.5}$ over the 13 measurement stations, the ref-VBS-GECKO parameterisation leads to an increase of the simulated concentration (+ 15.6 %), ultimately leading to a clear improvement of

10　MFE, MFB and correlation. Nevertheless, using the ref-VBS-GECKO configuration instead of the H^2O configuration increases RMSE (+5%), owing to a substantial overestimation of OA. The main differences between the two organic aerosol modules lie on OM_{PM1} with simulated ref-VBS-GECKO concentrations higher than H^2O by 31.5%. As simulated OM_{PM1} concentrations were highly underestimated using the former H^2O configuration compared to observations (6 stations), the ref-VBS-GECKO configuration improve RMSE, MFB and MFE.

15　Figure 3 shows comparisons between the measured and the simulated daily averaged temporal evolutions of OM_{PM1}, $OC_{PM2.5}$ and/or $PM_{2.5}$ concentrations at the 7 selected stations. Figure 4 shows the measured and simulated mean diurnal profiles at the 4 stations providing OM_{PM1}. Simulations capture qualitatively the observed feature of the daily averaged time series for $PM_{2.5}$, $OC_{PM2.5}$ and OM_{PM1}, and the mean diurnal profiles for OM_{PM1}. At stations dominantly impacted by biogenic sources, OA concentrations simulated with ref-VBS-GECKO are higher than those simulated with H^2O, leading to a better agreement

20　with measurements (see Fig. 3.d to h and Fig. 4.c and d). However, day/night variations of OM_{PM1} seem to be overstated. At stations influenced by anthropogenic air masses, OA concentrations are weakly influenced by the organic aerosol module (see Fig. 3.a to c and Fig. 4.a and b). OA concentrations simulated with ref-VBS-GECKO are substantially underestimated, differences exceeding -50% for OM_{PM1} concentrations at the FR0020R and DE0044R stations as well as for $OC_{PM2.5}$ concentrations at the NL0644R station.

25　**4.　Sensitivity to the parameterization properties**

Sensitivity tests were performed to assess the VBS-GECKO parameterization, evaluate the consistency of the modelling results and examine some hypotheses that may explain the gaps between measurement and simulated values. Sensitivities to hydro-solubility, gaseous ageing, NO_x regimes and volatility were studied comparing results to the non-modified ref-VBS-GECKO version.

4.1. Sensitivity tests to hydro-solubility and H^{eff}

SOA formation from the gas/particle partitioning of hydro-soluble organic compounds into an aqueous phase is now well recognized (e.g. Bregonzio-Rozier et al., 2016; Carlton et al., 2009; Knote et al., 2014). The effective Henry's law constant (H^{eff}) is the key parameter which controls this hydrophilic partitioning. Hydro-soluble organic compounds can also be lost at the surface by dry deposition. In CHIMERE, and according to the deposition scheme of Wesely (1989), the stomatal resistance of organic compounds depends on H^{eff}. To analyse the sensitivity of the simulated OA to hydrophilic partitioning and values of H^{eff}, the following two simulations were run:

- **Hydro-VBS-GECKO**. In this model configuration, VB(1-7) can condense on both organic and water phases of particles. Aqueous-phase partitioning is computed according to Henry's law, assuming the particle phase behave as an ideal well mixed homogeneous aqueous phase. Deposition of VB(1-7) was already taken into account in the reference model configuration and was kept unchanged.

- **Hydro-VBS-GECKO-high**. This model configuration is identical to the hydro-VBS-GECKO configuration above, except that the original H^{eff} of each VB are multiplied by 100. The new H^{eff} values correspond to the upper values of the H^{eff} distribution of secondary organic compounds contributing to a given volatility bin (see Lannuque et al., 2018).

The relative difference on the simulated mean OA concentrations between Hydro-VBS-GECKO (respectively Hydro-VBS-GECKO-high) and ref-VBS-GECKO is given Fig. 5.a (respectively Fig. 5.b) for the two-month period. Figure 5.a shows that considering aqueous phase partitioning of the VBS-GECKO species leads to variations on the simulated mean OA concentrations below ±0.5%. Table 4 shows no significant modification in the statistical results for this simulation. The values of H^{eff} set to each volatility bin increase when the volatility decreases (see Table 1), meaning that the less volatile species are also more prone to condense into the aqueous phase. Adding a hydrophilic partitioning does therefore not increase substantially the concentrations of organic species in the condensed phases.

The Hydro-VBS-GECKO-high configuration increases the mean simulated OA concentrations by ~10%, with a maximal increase reached over Benelux (~+20%, see Fig. 5.b). The contribution of the deposition and the partitioning processes are shown in Fig. 5.c and 5.d respectively. Changes due to deposition appear negligible (below ±0.2%) compared to the changes due to the aqueous partitioning (~+10%). According to the Wesely (1989) parameterization used for deposition, water solubility contributes to the surface resistance only. Knote et al. (2014) have shown that deposition is not limited by the surface resistance for H^{eff} greater than 10^8 mol L^{-1} atm^{-1}. In the ref-VBS-GECKO, this threshold corresponds to the VB(3-7) nominal H_{eff} values, i.e. to the volatility bins partitioning mainly to OA. OA concentrations are therefore not sensitive to an increase of the H_{eff} values. The increase of H^{eff} by a factor of 100 makes possible hydrophilic partitioning of the most volatile bins that would not have condensed otherwise and leads to an increase of simulated OA concentrations. The maximum relative changes simulated over Benelux are mainly linked to the high relative humidity encountered in this area and the low simulated OA concentrations (see Fig. 2.a). This model configuration improves slightly the RMSE, MFB and MFE

calculated on OM_{PM1} and $OC_{PM2.5}$ mass concentrations (see Table 4). According to these tests, SOA production due to the hydrophilic partitioning of the various VB(1-7) of the VBS-GECKO parameterization is expected to be a minor process.

4.2. Sensitivity test to ageing rates and OH radical concentrations

In the VBS-GECKO parameterization, the same rate constant is set for the VB(1-7) reactions with OH (k_{OH} = 4.0×10^{-11} cm^3

5   molec^{-1} s^{-1}). Timescale for aging is therefore driven by the OH concentrations simulated by the CTM. Simulated OH concentrations depend on the gas phase chemical mechanisms used in the CTM, with differences on OH concentrations reaching up to 45% between mechanisms (Sarwar et al., 2013). Two simulations were run with modified k_{OH} to examine the sensitivity of SOA production to the rate of chemical ageing:

- **k_{OH}-VBS-GECKO-low**. In this model configuration, the VB(1-7)+OH rate constants are divided by a factor 2, i.e.
10   k_{OH}^{low} = 2.0×10^{-11} cm^3 molec^{-1} s^{-1}.

- **k_{OH}-VBS-GECKO-high**. In this model configuration, the VB(1-7)+OH rate constants are multiplied by a factor 2, i.e. k_{OH}^{high} = 8.0×10^{-11} cm^3 molec^{-1} s^{-1}.

The relative difference on the simulated mean OA concentrations between k_{OH}-VBS-GECKO-low (respectively k_{OH}-VBS-GECKO-high) and ref-VBS-GECKO is given Fig. 6.a (respectively Fig. 6.b). A slight variation of simulated OA

15   concentrations is found (lower than ±10%), with simulated OA concentrations decreasing with the decrease of aging rates and *vice versa*. This result highlights that the gas-phase ageing of volatility bins in the VBS-GECKO parameterization promotes functionalization (formation of less volatile bins) rather than fragmentation (formation of more volatile bins), as already shown with tests conducted in box model (Lannuque et al., 2018). The highest relative differences are located over the Mediterranean Sea and North Africa, i.e. areas showing high OH and low OA concentrations (below 4 µg m^{-3}, see Fig.

20   2.a). The k_{OH}-VBS-GECKO-high configuration improves statistics, due to an overall increase of the simulated OA concentrations (and contrariwise for the k_{OH}-VBS-GECKO-low configuration) (see Table 4). However, the sensitivity of SOA to the gas-phase ageing of the volatility bins remains weak and aging rates is likely not a major source of uncertainty.

4.3. Sensitivity test to the NO$_x$ regime

Similar to the OH discussion above, simulated HO$_2$ and NO concentrations are provided by the CTM and are linked to the

25   gas phase chemical mechanism used. The concentrations of these two species determine the value of the RRR ratio and therefore drive the aging scheme for the various VB(1-7) (Lannuque et al., 2018). A sensitivity test was performed to examine the sensitivity of the simulated OA to the chemical regime. HO$_2$ or NO concentrations can hardly be modified without changing all the simulation conditions. Here, two simulations were run modifying the $k_{RO2+HO2}$ value used to calculate the RRR:

30   - **RRR-VBS-GECKO-low**. In this model configuration, RRR ratio is calculated with $k_{RO2+HO2}$ multiplied by 2, i.e. $k_{RO2+HO2}^{RRRlow}$ = 4.4×10^{-11} cm^3 molec^{-1} s^{-1}.

- **RRR-VBS-GECKO-high**. In this model configuration, RRR ratio is calculated with $k_{RO2+HO2}$ divided by 2, i.e. $k_{RO2+HO2}^{RRRhigh} = 1.1 \times 10^{-11}$ cm^3 molec^{-1} s^{-1}.

Figure 7 presents the mean RRR ratio during the two-month period for both RRR-VBS-GECKO-low (Fig. 7.a) and RRR-VBS-GECKO-high model configurations (Fig. 7.b). The entire range of RRR ratio (from free NO$_x$ to high NO$_x$ conditions) is

5 covered over Europe whatever the model configuration for RRR calculation. As expected, the urban, industrial and intense shipping transport areas such as Paris, the Channel, Benelux, northern Italy or Moscow are systematically in the high NO$_x$ regime (RRR close to 1) whereas remote areas over the seas (away from shipping tracks) are systematically in the NO$_x$ free regime (RRR close to 0). Between these two extremes, the RRR ratio depends on the environmental and meteorological conditions at the location and, in this sensitivity study, on the model configuration for the RRR calculation. Current

10 parameterizations for SOA formation only consider two extreme regimes corresponding to a high-NO$_x$ and a low-NO$_x$ condition. Criteria used to define high and low NO$_x$ differ from a study to another one but the parameterizations are usually optimized at NO$_x$ values typical of rural conditions for low NO$_x$ (corresponding to a RRR ratio of ~0.6) and typical of urban conditions for high NO$_x$ (corresponding to a RRR ratio of ~1) (e.g. Hodzic et al., 2014; Lane et al., 2008). The range of RRR between 0.0 and 0.6 is therefore not considered in most of the parameterizations, although substantial changes in SOA

15 formation were found within this range of RRR (Lannuque et al., 2018).

The relative difference on the simulated mean OA concentrations between RRR-VBS-GECKO-low (respectively RRR-VBS-GECKO-high) and ref-VBS-GECKO is given Fig. 8.a (respectively Fig. 8.b). Results show variations of simulated mean OA concentrations smaller than ~15%. In agreement with previous studies, an increase (decrease) of RRR ratio leads to a decrease (increase) of the simulated OA concentrations (e.g. Donahue et al., 2005; Lannuque et al., 2018; Ng et al., 2007).

20 As expected, the variation is weaker over areas having either an RRR ratio close to 0 or 1, the NO$_x$ regime remaining unchanged among the model configurations. The highest relative differences on OA are found over continental rural areas, i.e. areas showing the largest variation of RRR among model configurations. Large relative differences are also found over the Mediterranean Sea, owing in part to the low simulated OA concentrations. Similar to the k_{OH} sensitivity tests, the RRR-VBS-GECKO-low configuration increases the overall OA concentrations and improves statistical indicators, and

25 contrariwise for the RRR-VBS-GECKO-high configuration. Sensitivity on RRR values appears weak enough to likely not be a major source of uncertainty for the VBS-GECKO parameterization.

4.4. Sensitivity test to volatility and P^{sat}

The saturation vapour pressure, P^{sat}, of secondary organic compounds was estimated using structure activity relationships (SAR) (see Lannuque et al., 2018). Estimated P^{sat} can typically vary within one order of magnitude according to the SAR

30 used (e.g. Valorso et al., 2011). Two simulations were run to examine the sensitivity of SOA to the uncertainties in P^{sat}:

- **P^{sat}-VBS-GECKO-low.** In this model configuration, the nominal P^{sat} values of VB(1-7) are divided by 10.
- **P^{sat}-VBS-GECKO-high.** In this model configuration, the nominal P^{sat} values of VB(1-7) are multiplied by 10.

As OA concentration directly contributes to the partitioning, these two simulations can also be considered as a sensitivity test to the simulated OA concentrations.

The relative difference on the simulated mean OA concentrations between P^{sat}-VBS-GECKO-low (respectively P^{sat}-VBS-GECKO-high) and ref-VBS-GECKO is given Fig. 9.a (respectively Fig. 9.b). Shifting the volatility of the VB(1-7) by one

5　order of magnitude leads to an overall change in the simulated mean OA concentrations of about -25% (+25%) when P^{sat} is increased (decreased). A weaker sensitivity is observed over urban areas, such as Paris or Moscow. This behaviour is mainly linked to the simulated volatility of OA in the ref-VBS-GECKO simulations. Figure 10 shows the mean volatility of OA over Europe for the reference configuration. Simulated OA contributors are mainly low volatile species (with mean P^{sat}_{298K} between 10^{-10} and 10^{-14} atm), the highest values being found over urban areas (less aged OA), and the lowest values found

10　over areas close to the boundaries of the domain (linked to a boundary effect in the model). A shift in volatilities over these two types of site has a lower impact on OA concentrations, OA mean volatilities being either too high (mean $P^{sat}_{298K} \approx 10^{-10}$ atm, upon urban areas) or too low (mean $P^{sat}_{298K} \approx 10^{-14}$ atm, upon boundary areas) for a change in P^{sat} to substantially impact the partitioning. The largest effect is typically observed over central Europe where OA contributors show intermediate mean volatilities (mean $P^{sat}_{298K} \approx 10^{-12}$ atm).

15　Statistically, the P^{sat}-VBS-GECKO-low configuration is the only configuration matching the performance goal for all the simulated OA concentrations ($OC_{PM2.5}$ and OM_{PM1}) (see Table 4). For $OC_{PM2.5}$, RMSE is however higher than in reference configuration. Simulated OA concentrations appear to be sensitive to uncertainties in the estimated vapour pressures for the numerous OA contributors considered during the development of the VBS-GECKO parameterization.

5. Sensitivity to IVOC emissions from vehicle exhausts

20　IVOC have been shown to be a substantial source of SOA in the plume of megacities (e.g. Hodzic et al., 2010; Tsimpidi et al., 2010). A large fraction of these IVOC is expected to be first emitted in the condensed phase, and to rapidly volatilize with atmospheric dilution (Robinson et al., 2007). Robinson et al. (2007) assumed that IVOC emissions were equal to 150% of POA emissions, consistent with the Schauer et al. (1999) emission data for 1995 medium-duty diesel vehicles. Recent studies have measured IVOC emissions from (i) exhausts of a light-duty gasoline vehicle fleet and (ii) exhausts of both

25　heavy-duty and medium-duty diesel vehicle fleets (Zhao et al., 2015, 2016). Experiments on gasoline vehicles have been processed on a 42 vehicle fleet and experiments on diesel vehicles have been processed on 6 vehicles representative of the transportation fleet in North America. In both cases, Zhao et al. (2015, 2016) have shown that a stronger correlation can be found between IVOC and VOC emissions (R^2 equal to 0.92 and 0.98 for gasoline and diesel exhausts, respectively) than between IVOC and POA emissions (R^2 equal to 0.76 and 0.61 for gasoline and diesel exhausts, respectively). Zhao et al.

30　(2015, 2016) have estimated that IVOC emissions represent about 4% of NMVOC emissions in cold-start cycle to about 16% in hot-start cycle for light-duty gasoline vehicles, and about 60 ± 10 % of NMVOC emissions for heavy-duty and medium-duty diesel vehicles.

Atmospheric
Chemistry
and Physics
Discussions

In this study, the VBS-GECKO parameterization was used to examine the sensitivity of SOA to IVOC emissions from traffic and transport (SNAP 7 and 8). The following five model configurations, based on different emission scenarios, were designed for that purpose:

- **IVOC$_{150POA}$.** In this model configuration, IVOC emissions are set to 150% of the POA emissions, based on
5   Robinson et al. (2007).

- **IVOC$_{4VOC}$.** In this configuration, IVOC emissions are set to 4% of NMVOC emissions, based on Zhao et al. (2016) for gasoline vehicles in cold-start cycle.

- **IVOC$_{16VOC}$.** In this configuration, IVOC emissions are set to 16% of NMVOC emissions, based on Zhao et al. (2016) for gasoline vehicles in hot-start cycle.

10 - **IVOC$_{30VOC}$.** In this configuration, emissions are set to 30% of NMVOC emissions, assuming a mixing of diesel and gasoline vehicle fleets.

- **IVOC$_{65VOC}$.** In this configuration, IVOC emissions are set to 65% of NMVOC emissions, based on Zhao et al. (2015) for diesel vehicles.

As in the reference model configuration, POA are distributed into SVOC with a SVOC/POA ratio of 1 in these sensitivity
15 tests for traffic and transport emissions. SVOC and IVOC constitute a complex mixture of linear, branched and cyclic alkanes, alkenes and aromatics (Fraser et al., 1997; Gentner et al., 2012; Schauer et al., 1999, 2002). The molecular composition of S/IVOC emitted in the atmosphere by fossil fuel combustion is however still poorly documented. S/IVOC at emission were thus considered to be distributed into the 9 volatility bins given by Robinson et al. (2007), with the provided fraction of SVOC in each SVOC volatility bin, and of IVOC in each IVOC volatility bin. The VBS-GECKO
20 parameterizations for C_{14}, C_{18}, C_{22} and C_{26} 1-alkenes and n-alkanes were used as surrogate mechanisms for S/IVOC. The C_{14} to C_{26} VBS-GECKO's n-alkanes and 1-alkenes were distributed according to their volatility into the 9 volatility bins of Robinson et al. (2007). Correspondences are shown in Figure 11, for the example of the IVOC$_{150POA}$ model configuration. The distribution of alkanes and alkenes was estimated based on (i) the EMEP guidebook (https://www.eea.europa.eu/publications/emep-eea-guidebook-2016), providing speciation data for emissions for various
25 types of vehicles and (ii) the COPERT4 software (Ntziachristos et al., 2009) providing data for a vehicle fleet. Data are only available for light compounds and are here extrapolated to the heavy ones for the needs of the study. Thus, 75 % of the S/IVOC species are here assumed to be alkanes and 25 % alkenes. The SVOC total emissions and distributions over volatility bins are unchanged between each simulation. The distribution of IVOC among volatility bins is also unchanged but the total IVOC emissions are modulated according to the assumptions on IVOC emissions. Table 5 gives the speciation of
30 VBS-GECKO species for the various model configurations and the VBS-GECKO mechanism for S/IVOC is presented in Table S3 of supplementary material.

Figure 12 shows the mean OA mass concentrations simulated for the 5 IVOC emission configurations, and the absolute and relative differences with the ref-VBS-GECKO simulation without IVOC emissions. Table 6 presents the statistical results

calculated on daily averaged concentrations (RMSE, correlation coefficients, MFE and MFB) for the different IVOC emission configurations, and their difference with those of the ref-VBS-GECKO configuration. As discussed previously, the highest concentrations are simulated over northern Italy (see Fig. 2). For this area, accounting for IVOC emissions increases the simulated concentrations of OA up to 3 µg m^{-3} with the IVOC$_{65VOC}$ model configuration. As expected, OA concentration

5   increases when IVOC emissions over Europe are taken into account during the simulated period, with an overall mean increase of about 2, 5, 10 and 20% for the IVOC$_{4VOC}$, IVOC$_{16VOC}$, IVOC$_{30VOC}$ and IVOC$_{65VOC}$ configuration, respectively. The relative differences show large increases of OA concentrations (reaching +40%) over a large area including North Sea and Benelux for the IVOC$_{65VOC}$ configuration, owing to the low simulated OA concentrations with the ref-VBS-GECKO configuration. The IVOC$_{150POA}$ configuration leads to mean OA mass concentrations lying between the IVOC$_{16VOC}$ and the

10   IVOC$_{30VOC}$ configurations. Area showing substantial changes in simulated OA are however different between these model configurations. In the IVOC$_{150POA}$ configuration, the largest OA increase is simulated over the Channel and Gibraltar's Detroit (up to +80%). These results were expected for this model configuration based on POA emissions. Indeed, ships are one of the most important emitter of POA but emit a relatively small amount of NMVOC. For example, the EMEP inventory for 2013 estimates an average NMVOC/POA emission ratio of ~4 for road traffic in Europe and ~0.4 for shipping in the

15   studied domain.

Taking into account SOA formation from IVOC precursors improves the statistical indicators for the simulated concentrations of OM$_{PM1}$. As discussed previously, the ref-VBS-GECKO configuration underestimates OM$_{PM1}$. Including IVOC emission increases the mean OM$_{PM1}$ concentrations at the stations of about 5, 2, 5, 7 or 13% for the IVOC$_{150POA}$, IVOC$_{4VOC}$, IVOC$_{16VOC}$, IVOC$_{30VOC}$ or IVOC$_{65VOC}$ configuration, respectively. Increasing IVOC emissions provide better

20   statistical indicators for OM$_{PM1}$, with MFE and MFB significantly closer to the performance goal (MFE decreases by 0.06 and |MFB| decreases by 0.09 between IVOC$_{4VOC}$ and IVOC$_{65VOC}$ configurations, see Table 6). For OC$_{PM2.5}$ however, the opposite trend is observed with a degradation of the statistical indicators (Table 6). The ref-VBS-GECKO configuration leads to a slight overestimation of OC$_{PM2.5}$ concentrations over some stations (e.g. SI0008R, see Fig. 3) and adding the SOA source from IVOC strengthens the deviation (up to about +30% of RMSE for the IVOC$_{65VOC}$ configuration), even if the

25   correlation is not significantly modified.

IVOC oxidation appears to be a significant SOA source at some locations (e.g. the NL0644R station), especially in the IVOC$_{30VOC}$ and IVOC$_{65VOC}$ configuration. However, the resulting OA increase remains too weak to fill in the gaps between observations and simulated data (maximum increase around +40%). For example, time series presented in Figure 13 show that adding IVOC emission increases systematically the simulated OA concentrations, but not enough to explain the OA

30   peaks recorded at the anthropogenic stations (see Fig. 13.b). Moreover, accounting for IVOC emission strengthens the disagreement of the simulated concentrations with observations over other areas (e.g. at SI0008R station).

The various IVOC configurations are aimed to represent different vehicle fleet, from a heavy diesel to a light gasoline vehicle fleet (see above). At a local scale, IVOC emissions from road traffic appear to be a significant source of OA and OA concentrations are dependant to the European fleet type. At a continental scale, the slight variations observed on simulated

Atmospheric
Chemistry
and Physics
Discussions

OA concentrations suggest that IVOC from road traffic are likely not a major source of SOA, whatever the engine nature of the vehicle fleet.

6. Tracking OA sources

Apportionment of OA sources is investigated in this section. The study takes into account OA formation from IVOC
5   oxidation and is based on the IVOC$_{30VOC}$ model configuration. Figure 14 shows the contribution of the various OA sources to the simulated OA concentrations during the July-August 2013 period and the mean daily profiles at two stations located in areas dominantly impacted by anthropogenic air masses (NL0644R and FR0020R) and two stations located in areas dominantly impacted by biogenic air masses (NO0002R and SI0008R). SOA constitutes the main fraction of OA whatever the environment. This secondary fraction typically grows from anthropogenic impacted areas (about 70 % at FR0020R
10   station) to remote areas (about 95 % at SI0008R station). This trend is in agreement with what is usually observed or simulated for summertime periods (e.g. Aksoyoglu et al. 2011; Belis et al., 2013). For the remote stations NO0002R and SI0008R, respectively 82 and 67% of the simulated OA concentration comes from a biogenic source. Contrariwise, anthropogenic sources are the major OA contributors at anthropogenic impacted stations (65 and 60% of OA at the NL0644R and FR0020R stations, respectively.
15   Among OA biogenic sources, terpene oxidation is clearly found as the major contributor of OA during the summer period, contributing from 35% (at anthropogenic impacted stations) to 80% (at remote stations) of the total OA mass. The 60% increase of OA mass concentration observed in north Europe between H^{2}O and VBS-GECKO parameterizations (see Fig. 2) is also mainly related to SOA formation from terpene, especially ocimene and limonene. In our simulation, SOA produced by isoprene oxidation does not represent a substantial fraction of OA at the selected measurement stations. The major
20   contribution of isoprene SOA to OA reached about 5% (see Fig. 14.h) and is observed at the SI0008R station during diurnal conditions.

The anthropogenic fraction of OA is found to be dominated by residential biomass burning sources (BBOA). Indeed, according to the temporal factors used in CHIMERE (based on GENEMIS, Ebel et al., 1997; Friedrich, 2000), 4% of annual emissions of residential BBOA occurs during July-August, leading to a non-negligible amount of residential BBOA during
25   summer. This result remains however subject to caution, owing to the large uncertainties in the temporalization of biomass burning emissions in the model. The primary organic fraction (i.e. condensed primary SVOC) from traffic emissions is found to be substantial in the OA budget only at night in urban areas. On the other hand, the secondary organic fraction produced by traffic emissions can represent about 50% of diurnal anthropogenic OA at stations near urban areas (i.e. FR0020R and NL0664R). OA formed by the oxidation of mono-aromatic species is found to be negligible over Europe (less than 0.025 µg
30   m^{-3} on average over the studied domain). Figure 15 shows the contribution of traffic emission to the simulated OA concentrations for the July-August 2013 period for 3 categories of precursors: SVOC, IVOC and mono-aromatic compounds. As mentioned above, the OA concentrations from mono-aromatic compound oxidation are negligible compared

to concentrations from traffic S/IVOC oxidation. Globally, in our study over Europe, OA concentrations produced from traffic IVOC and SVOC oxidation are of the same order of magnitude. OA from SVOC is locally more important close to sources (i.e. Northern Italy, Moscow, Paris, Gibraltar, etc). OA from IVOC is globally higher far away from the sources, with a higher dispersion over Europe (Fig. 15). This higher dispersion is expected owing to the larger timescale required to

5 produce low volatility species via multistep oxidation processes in the plumes of high emission area.

The distributions of OA within the volatility bins (given in Figure S2 of supplementary material) show similar features from one station to another. The results suggest that OA over Europe have relatively low volatility during summertime. Indeed, the VBS-GECKO contributors to OA have very low volatility: ~80% of the OA from VBS-GECKO are volatility bins 7 to 5 (VB7, VB6 and VB5 species), i.e. having vapour pressure at 298 K of 10^{-14}, 10^{-12} and 10^{-11} atm respectively.

10

7. Conclusions

The VBS-GECKO parameterization for SOA production has been developed based on explicit mechanisms generated with the GECKO-A tool. The VBS-GECKO parameterization was fitted using box modelling results for a selected set of parent compounds including terpenes, mono-aromatic compounds, linear alkanes and alkenes and for various environmental

15 conditions, including different NO_x regimes, temperatures, OA loads (Lannuque et al., 2018). In this study, the VBS-GECKO parameterization was evaluated in the CHIMERE β 2017 CTM over Europe during summertime.

The VBS-GECKO parameterization shows good performances to simulate OA concentrations over Europe in the summer. Calculated mean fractional bias and mean fractional error on $PM_{2.5}$, $OC_{PM2.5}$ and OM_{PM1} satisfy performance criteria of Boylan and Russel (2006). The model configuration including the VBS-GECKO parameterization yields to higher OA

20 concentrations compared to the former reference configuration including the H^2O parameterization. The deviations between the two configurations are especially marked over northern Europe, with an increase factor of ~60%. Outside this area, the OA increases obtained with the VBS-GECKO configuration are slight. Statistically, using the VBS-GECKO improves the overall MFB, MFE and RMSE and does not modify significantly correlation coefficients. Tests performed to examine the sensitivity of simulated OA concentrations to hydro-solubility, volatility, ageing rates and NO_x regimes have shown that the

25 VBS-GECKO parameterization provides consistent results that are not subject to large deviations induced by parameters provided by the gas phase mechanism included in the CTM (e.g. HO_x or NO_x concentrations). However, the OA concentrations remain underestimated with the VBS-GECKO model configuration, especially in areas with a significant contribution of anthropogenic sources (e.g. reaching a factor of 2.5 for $OC_{PM2.5}$ at the NL0644R station in Netherlands). None of the conducted sensitivity test leads to OA variations large enough to fill the gaps between measurements and

30 simulated concentrations at the anthropogenic stations.

The analysis of simulated OA shows that, during summertime, the main fraction is made of secondary matter which represents ~85% of the total mean OA concentration. A large fraction of the simulated OA comes from biogenic sources

(between 30 and 85% of the total OA), especially from terpene oxidation which represents ~95% of these biogenic sources. For the conditions examined in this study, OA formed by the oxidation of mono-aromatic compounds appears to be negligible with maximum mean concentrations of 0.025 µg m^{-3} over North Sea and Benelux. Note that ignoring SOA production from these precursors in the model would substantially reduce the number of VB(1-7) species currently

5　considered in the VBS-GECKO parameterization. The simulated OA was found to be made of species having low and extremely low volatilities (LVOC and ELVOC) in remote areas, but also of SVOC closer to major anthropogenic sources. Finally, IVOC oxidation was added to examine the contribution of this additional source to the SOA budget. Five model configurations with distinct IVOC emissions from traffic were tested and compared using the VBS-GECKO parameterization in CHIMERE. These model configurations aimed to represent various vehicle fleets (from heavy diesel to

10　light gasoline fleets). As expected, considering the emission of IVOC by surface transportation was found to globally increase background OA concentrations. Although SOA production from traffic IVOC oxidation can locally be significant (up to ~+3 µg m^{-3} in northern Italy, assuming a full diesel fleet), this additional OA source remains too small to explain the gap between simulated and measured values at stations where anthropogenic sources are dominant. This first application of this new VBS-GECKO parameterization has been shown to provide consistent results. This outcome create motivation to

15　extend the exploration to wintertime conditions, and expand the list of parent compounds considered, in particular to include SOA formation from oxidation of isoprene, sesquiterpenes or organics species emitted by residential biomass burning, a prerequisite to extend the evaluation and analysis to wintertime when this source is dominant. This is the subject of ongoing studies. The VBS-GECKO is a heavy parameterization in term of species number. Calculation time is multiplied by two using the complete VBS-GECKO scheme with IVOC compared to H^{2}O. This study has revealed that the number of species

20　can be optimized. For example, because of the low OA concentrations formed, the representation of the SOA formed by the oxidation of mono-aromatic species can be highly simplified and C$_{10}$ precursors even removed.

Data availability

Daily averages and mean day profiles for the 17 model configurations presented in this article have been made available on Zenodo: https://zenodo.org/record/ 1654297 / (last access: 29 November 2018).

25　**Competing interests**

The authors declare that they have no conflict of interest.

Atmospheric
Chemistry
and Physics
Discussions

Open Access

EGU

Author Contribution

VL implemented the parameterization in the air quality model and conducted the simulations and the sensitivity tests. All the authors contributed to design the research, to interpret the data and to write the article.

References

10   Aksoyoglu, S., Keller, J., Barmpadimos, I., Oderbolz, D., Lanz, V. A., Prévăt, A. S. H. and Baltensperger, U.: Aerosol modelling in Europe with a focus on Switzerland during summer and winter episodes, Atmos. Chem. Phys., 11(14), 7355–7373, https://doi.org/10.5194/acp-11-7355-2011, 2011.

Aumont, B., Szopa, S. and Madronich, S.: Modelling the evolution of organic carbon during its gas-phase tropospheric oxidation: development of an explicit model based on a self generating approach, Atmos. Chem. Phys., 5(9), 2497–2517,
15   https://doi.org/10.5194/acp-5-2497-2005, 2005.

Belis, C. A., Karagulian, F., Larsen, B. R. and Hopke, P. K.: Critical review and meta-analysis of ambient particulate matter source apportionment using receptor models in Europe, Atmos. Environ., 69, 94–108, https://doi.org/10.1016/j.atmosenv.2012.11.009, 2013.

Bessagnet, B., Hodzic, A., Vautard, R., Beekmann, M., Cheinet, S., Honoré, C., Liousse, C. and Rouil, L.: Aerosol modeling
20   with CHIMERE - Preliminary evaluation at the continental scale, Atmos. Environ., 38(18), 2803–2817, https://doi.org/10.1016/j.atmosenv.2004.02.034, 2004.

Bessagnet, B., Menut, L., Curci, G., Hodzic, A., Guillaume, B., Liousse, C., Moukhtar, S., Pun, B., Seigneur, C. and Schulz, M.: Regional modeling of carbonaceous aerosols over Europe—focus on secondary organic aerosols, J. Atmos. Chem., 61(3), 175–202, https://doi.org/10.1007/s10874-009-9129-2, 2009.

25   Bessagnet, B., Seigneur, C. and Menut, L.: Impact of dry deposition of semi-volatile organic compounds on secondary organic aerosols, Atmos. Environ., 44(14), 1781–1787, https://doi.org/10.1016/j.atmosenv.2010.01.027, 2010.

Bessagnet, B., Pirovano, G., Mircea, M., Cuvelier, C., Aulinger, A., Calori, G., Ciarelli, G., Manders, A., Stern, R., Tsyro, S., Garciá Vivanco, M., Thunis, P., Pay, M. T., Colette, A., Couvidat, F., Meleux, F., Rouïl, L., Ung, A., Aksoyoglu, S., Baldasano, J. M., Bieser, J., Briganti, G., Cappelletti, A., D'Isidoro, M., Finardi, S., Kranenburg, R., Silibello, C., Carnevale,
30   C., Aas, W., Dupont, J. C., Fagerli, H., Gonzalez, L., Menut, L., Prévôt, A. S. H., Roberts, P. and White, L.: Presentation of

the EURODELTA III intercomparison exercise-evaluation of the chemistry transport models' performance on criteria pollutants and joint analysis with meteorology, Atmos. Chem. Phys., 16(19), 12667–12701, https://doi.org/10.5194/acp-16-12667-2016, 2016.

Boucher, O., Randall, D., Artaxo, P., Bretherton, C., Feingold, G., Forster, P., Kerminen, V.-M., Kondo, Y., Liao, H.,
5 Lohmann, U., Rasch, P., Satheesh, S. K., Sherwood, S., Stevens, B. and Zhang, X. Y.: Clouds and Aerosols, in Climate Change 2013 - The Physical Science Basis. Contribution of Working Group I to the Fifth Assessment Report of the Intergovernmental Panel on Climate Change, edited by T. F. Stocker, D. Qin, G.-K. Plattner, M. Tignor, S. K. Allen, J. Boschung, A. Nauels, Y. Xia, V. Bex, and P. M. Midgley, pp. 571–658, Cambridge University Press, Cambridge, United Kingdom and New York, NY, USA., 2013.

10 Boylan, J. W. and Russell, A. G.: PM and light extinction model performance metrics, goals, and criteria for three-dimensional air quality models, Atmos. Environ., 40(26), 4946–4959, https://doi.org/10.1016/j.atmosenv.2005.09.087, 2006.

Bregonzio-Rozier, L., Giorio, C., Siekmann, F., Pangui, E., Morales, S. B., Temime-Roussel, B., Gratien, A., Michoud, V., Cazaunau, M., Dewitt, H. L., Tapparo, A., Monod, A. and Doussin, J. F.: Secondary organic aerosol formation from isoprene photooxidation during cloud condensation-evaporation cycles, Atmos. Chem. Phys., 16(3), 1747–1760,
15 https://doi.org/10.5194/acp-16-1747-2016, 2016.

Camredon, M., Aumont, B., Lee-Taylor, J. and Madronich, S.: The SOA/VOC/NOx system: an explicit model of secondary organic aerosol formation, Atmos. Chem. Phys., 7(21), 5599–5610, https://doi.org/10.5194/acp-7-5599-2007, 2007.

Canagaratna, M. R., Jimenez, J. L., Kroll, J. H., Chen, Q., Kessler, S. H., Massoli, P., Hildebrandt Ruiz, L., Fortner, E., Williams, L. R., Wilson, K. R., Surratt, J. D., Donahue, N. M., Jayne, J. T. and Worsnop, D. R.: Elemental ratio
20 measurements of organic compounds using aerosol mass spectrometry: Characterization, improved calibration, and implications, Atmos. Chem. Phys., 15(1), 253–272, https://doi.org/10.5194/acp-15-253-2015, 2015.

Cappa, C. D., Jathar, S. H., Kleeman, M. J., Docherty, K. S., Jimenez, J. L., Seinfeld, J. H. and Wexler, A. S.: Simulating secondary organic aerosol in a regional air quality model using the statistical oxidation model - Part 2: Assessing the influence of vapor wall losses, Atmos. Chem. Phys., 16(5), 3041–3059, https://doi.org/10.5194/acp-16-3041-2016, 2016.

25 Carlton, A. G., Wiedinmyer, C. and Kroll, J. H.: A review of Secondary Organic Aerosol (SOA) formation from isoprene, Atmos. Chem. Phys., 9(14), 4987–5005, https://doi.org/10.5194/acp-9-4987-2009, 2009.

Carter, W. P. L.: A detailed mechanism for the gas-phase atmospheric reactions of organic compounds, Atmos. Environ., 24(3), 481–518, https://doi.org/10.1016/0960-1686(90)90005-8, 1990.

Ciarelli, G., Aksoyoglu, S., Crippa, M., Jimenez, J. L., Nemitz, E., Sellegri, K., Äijälä, M., Carbone, S., Mohr, C., O'dowd,
30 C., Poulain, L., Baltensperger, U. and Prévôt, A. S. H.: Evaluation of European air quality modelled by CAMx including the volatility basis set scheme, Atmos. Chem. Phys., 16(16), 10313–10332, https://doi.org/10.5194/acp-16-10313-2016, 2016.

Couvidat, F. and Sartelet, K.: The Secondary Organic Aerosol Processor (SOAP v1.0) model: a unified model with different ranges of complexity based on the molecular surrogate approach, Geosci. Model Dev., 8(4), 1111–1138, https://doi.org/10.5194/gmd-8-1111-2015, 2015.

Couvidat, F. and Seigneur, C.: Modeling secondary organic aerosol formation from isoprene oxidation under dry and humid conditions, Atmos. Chem. Phys., 11(2), 893–909, https://doi.org/10.5194/acp-11-893-2011, 2011.

Couvidat, F., Debry, É., Sartelet, K. and Seigneur, C.: A hydrophilic/hydrophobic organic (H2O) aerosol model: Development, evaluation and sensitivity analysis, J. Geophys. Res., 117(D10), D10304, https://doi.org/10.1029/2011JD017214, 2012.

Couvidat, F., Kim, Y., Sartelet, K., Seigneur, C., Marchand, N. and Sciare, J.: Modeling secondary organic aerosol in an urban area: Application to Paris, France, Atmos. Chem. Phys., 13(2), 983–996, https://doi.org/10.5194/acp-13-983-2013, 2013.

Couvidat, F., Bessagnet, B., Garcia-Vivanco, M., Real, E., Menut, L. and Colette, A.: Development of an inorganic and organic aerosol model (CHIMERE 2017β v1.0): seasonal and spatial evaluation over Europe, Geosci. Model Dev., 11(1), 165–194, https://doi.org/10.5194/gmd-11-165-2018, 2018.

Crippa, M., Canonaco, F., Lanz, V. A., Äijälä, M., Allan, J. D., Carbone, S., Capes, G., Ceburnis, D., Dall'Osto, M., Day, D. A., DeCarlo, P. F., Ehn, M., Eriksson, A., Freney, E., Ruiz, L. H., Hillamo, R., Jimenez, J. L., Junninen, H., Kiendler-Scharr, A., Kortelainen, A. M., Kulmala, M., Laaksonen, A., Mensah, A. A., Mohr, C., Nemitz, E., O'Dowd, C., Ovadnevaite, J., Pandis, S. N., Petäjä, T., Poulain, L., Saarikoski, S., Sellegri, K., Swietlicki, E., Tiitta, P., Worsnop, D. R., Baltensperger, U. and Prévôt, A. S. H.: Organic aerosol components derived from 25 AMS data sets across Europe using a consistent ME-2 based source apportionment approach, Atmos. Chem. Phys., 14(12), 6159–6176, https://doi.org/10.5194/acp-14-6159-2014, 2014.

Debry, E., Fahey, K., Sartelet, K., Sportisse, B. and Tombette, M.: Technical Note: A new SIze REsolved Aerosol Model (SIREAM), Atmos. Chem. Phys., 7(6), 1537–1547, https://doi.org/10.5194/acp-7-1537-2007, 2007.

Denier Van Der Gon, H. A. C., Bergström, R., Fountoukis, C., Johansson, C., Pandis, S. N., Simpson, D. and Visschedijk, A. J. H.: Particulate emissions from residential wood combustion in Europe - revised estimates and an evaluation, Atmos. Chem. Phys., 15(11), 6503–6519, https://doi.org/10.5194/acp-15-6503-2015, 2015.

Denkenberger, K. A., Moffet, R. C., Holecek, J. C., Rebotier, T. P. and Prather, K. A.: Real-time, single-particle measurements of oligomers in aged ambient aerosol particles, Environ. Sci. Technol., 41(15), 5439–5446, https://doi.org/10.1021/es070329l, 2007.

Dommen, J., Metzger, A., Duplissy, J., Kalberer, M., Alfarra, M. R., Gascho, A., Weingartner, E., Prevot, A. S. H., Verheggen, B. and Baltensperger, U.: Laboratory observation of oligomers in the aerosol from isoprene/NO x photooxidation, Geophys. Res. Lett., 33(13), 1–5, https://doi.org/10.1029/2006GL026523, 2006.

Donahue, N. M., Huff Hartz, K. E., Chuong, B., Presto, A. A., Stanier, C. O., Rosenhorn, T., Robinson, A. L. and Pandis, S. N.: Critical factors determining the variation in SOA yields from terpene ozonolysis: A combined experimental and computational study, Faraday Discuss., 130, 295–309, https://doi.org/10.1039/b417369d, 2005.

Donahue, N. M., Robinson, a. L., Stanier, C. O. and Pandis, S. N.: Coupled partitioning, dilution, and chemical aging of semivolatile organics, Environ. Sci. Technol., 40(8), 2635–2643, https://doi.org/10.1021/es052297c, 2006.

Donahue, N. M., Kroll, J. H., Pandis, S. N. and Robinson, A. L.: A two-dimensional volatility basis set – Part 2: Diagnostics of organic-aerosol evolution, Atmos. Chem. Phys., 12(2), 615–634, https://doi.org/10.5194/acp-12-615-2012, 2012.

Ebel, A., Friedrich, R. and Rodhe, H.: GENEMIS: Assessment, Improvement, and Temporal and Spatial Disaggregation of European Emission Data, in Tropospheric Modelling and Emission Estimation, pp. 181–214, Springer Berlin Heidelberg, Berlin, Heidelberg., 1997.

5   Emmons, L. K., Walters, S., Hess, P. G., Lamarque, J.-F., Pfister, G. G., Fillmore, D., Granier, C., Guenther, A., Kinnison, D., Laepple, T., Orlando, J., Tie, X., Tyndall, G., Wiedinmyer, C., Baughcum, S. L. and Kloster, S.: Description and evaluation of the Model for Ozone and Related chemical Tracers, version 4 (MOZART-4), Geosci. Model Dev., 3(1), 43–67, https://doi.org/10.5194/gmd-3-43-2010, 2010.

10   Fountoukis, C. and Nenes, A.: ISORROPIA II: a computationally efficient thermodynamic equilibrium model for $K^+–Ca^{2+}–Mg^{2+}–NH_4^+–Na^+–SO_4^{2-}–NO_3^-$, Atmos. Chem. Phys., 7(17), 4639–4659, https://doi.org/10.5194/acp-7-4639-2007, 2007.

Fraser, M., Cass, G., Simoneit, B. and Rasmussen, R.: Air quality model evaluation data for organics .4. C2-C36 non-aromatic hydrocarbons, Environ. Sci. Technol., 31(8), 2356–2367, https://doi.org/10.1021/es960980g, 1997.

15   Friedrich, R.: GENEMIS: Generation of European Emission Data for Episodes, in Transport and Chemical Transformation of Pollutants in the Troposphere, pp. 375–386, Springer Berlin Heidelberg, Berlin, Heidelberg., 2000.

Gelencsér, A., May, B., Simpson, D., Sánchez-Ochoa, A., Kasper-Giebl, A., Puxbaum, H., Caseiro, A., Pio, C. and Legrand, M.: Source apportionment of PM2.5 organic aerosol over Europe: Primary/secondary, natural/anthropogenic, and fossil/biogenic origin, J. Geophys. Res., 112(D23), D23S04, https://doi.org/10.1029/2006JD008094, 2007.

20   Gentner, D. R., Isaacman, G., Worton, D. R., Chan, A. W. H., Dallmann, T. R., Davis, L., Liu, S., Day, D. A., Russell, L. M., Wilson, K. R., Weber, R., Guha, A., Harley, R. A. and Goldstein, A. H.: Elucidating secondary organic aerosol from diesel and gasoline vehicles through detailed characterization of organic carbon emissions, Proc. Natl. Acad. Sci., 109(45), 18318–18323, https://doi.org/10.1073/pnas.1212272109/-/DCSupplemental.www.pnas.org/cgi/doi/10.1073/pnas.1212272109, 2012.

25   de Gouw, J. A., Middlebrook, A. M., Warneke, C., Goldan, P. D., Kuster, W. C., Roberts, J. M., Fehsenfeld, F. C., Worsnop, D. R., Canagaratna, M. R., Pszenny, A. A. P., Keene, W. C., Marchewka, M., Bertman, S. B. and Bates, T. S.: Budget of organic carbon in a polluted atmosphere: Results from the New England Air Quality Study in 2002, J. Geophys. Res., 110(D16), D16305, https://doi.org/10.1029/2004JD005623, 2005.

Guenther, A. B., Jiang, X., Heald, C. L., Sakulyanontvittaya, T., Duhl, T., Emmons, L. K. and Wang, X.: The model of 30   emissions of gases and aerosols from nature version 2.1 (MEGAN2.1): An extended and updated framework for modeling biogenic emissions, Geosci. Model Dev., 5(6), 1471–1492, https://doi.org/10.5194/gmd-5-1471-2012, 2012.

Han, S., Bian, H., Zhang, Y., Wu, J., Wang, Y., Tie, X., Li, Y., Li, X. and Yao, Q.: Effect of Aerosols on Visibility and Radiation in Spring 2009 in Tianjin, China, Aerosol Air Qual. Res., 12, 211–217, https://doi.org/10.4209/aaqr.2011.05.0073, 2012.

Atmospheric
Chemistry
and Physics
Discussions

Heald, C. L., Jacob, D. J., Park, R. J., Russell, L. M., Huebert, B. J., Seinfeld, J. H., Liao, H. and Weber, R. J.: A large organic aerosol source in the free troposphere missing from current models, Geophys. Res. Lett., 32(18), n/a-n/a, https://doi.org/10.1029/2005GL023831, 2005.

Hodzic, A., Jimenez, J. L., Madronich, S., Canagaratna, M. R., DeCarlo, P. F., Kleinman, L. and Fast, J.: Modeling organic
5 aerosols in a megacity: potential contribution of semi-volatile and intermediate volatility primary organic compounds to secondary organic aerosol formation, Atmos. Chem. Phys., 10(12), 5491–5514, https://doi.org/10.5194/acp-10-5491-2010, 2010.

Hodzic, A., Aumont, B., Knote, C., Lee-Taylor, J., Madronich, S. and Tyndall, G.: Volatility dependence of Henry's law constants of condensable organics: Application to estimate depositional loss of secondary organic aerosols, Geophys. Res.
10 Lett., 41(13), 4795–4804, https://doi.org/10.1002/2014GL060649, 2014.

Im, U., Bianconi, R., Solazzo, E., Kioutsioukis, I., Badia, A., Balzarini, A., Baró, R., Bellasio, R., Brunner, D., Chemel, C., Curci, G., Flemming, J., Forkel, R., Giordano, L., Jiménez-Guerrero, P., Hirtl, M., Hodzic, A., Honzak, L., Jorba, O., Knote, C., Kuenen, J. J. P., Makar, P. A., Manders-Groot, A., Neal, L., Pérez, J. L., Pirovano, G., Pouliot, G., San Jose, R., Savage, N., Schroder, W., Sokhi, R. S., Syrakov, D., Torian, A., Tuccella, P., Werhahn, J., Wolke, R., Yahya, K., Zabkar, R., Zhang,
15 Y., Zhang, J., Hogrefe, C. and Galmarini, S.: Evaluation of operational on-line-coupled regional air quality models over Europe and North America in the context of AQMEII phase 2. Part I: Ozone, Atmos. Environ., 115, 404–420, https://doi.org/10.1016/j.atmosenv.2014.09.042, 2015.

Jacobson, M. Z., Turco, R. P., Jensen, E. J. and Toon, O. B.: Modeling coagulation among particles of different composition and size, Atmos. Environ., 28(7), 1327–1338, https://doi.org/10.1016/1352-2310(94)90280-1, 1994.
20 Jimenez, J. L., Canagaratna, M. R., Donahue, N. M., Prevot, A. S. H., Zhang, Q., Kroll, J. H., DeCarlo, P. F., Allan, J. D., Coe, H., Ng, N. L., Aiken, A. C., Docherty, K. S., Ulbrich, I. M., Grieshop, A. P., Robinson, A. L., Duplissy, J., Smith, J. D., Wilson, K. R., Lanz, V. A., Hueglin, C., Sun, Y. L., Tian, J., Laaksonen, A., Raatikainen, T., Rautiainen, J., Vaattovaara, P., Ehn, M., Kulmala, M., Tomlinson, J. M., Collins, D. R., Cubison, M. J., Dunlea, E. J., Huffman, J. A., Onasch, T. B., Alfarra, M. R., Williams, P. I., Bower, K., Kondo, Y., Schneider, J., Drewnick, F., Borrmann, S., Weimer, S., Demerjian, K.,
25 Salcedo, D., Cottrell, L., Griffin, R., Takami, A., Miyoshi, T., Hatakeyama, S., Shimono, A., Sun, J. Y., Zhang, Y. M., Dzepina, K., Kimmel, J. R., Sueper, D., Jayne, J. T., Herndon, S. C., Trimborn, A. M., Williams, L. R., Wood, E. C., Middlebrook, A. M., Kolb, C. E., Baltensperger, U. and Worsnop, D. R.: Evolution of organic aerosols in the atmosphere., Science (80-.)., 326(5959), 1525–9, https://doi.org/10.1126/science.1180353, 2009.

Johnson, D., Utembe, S. R., Jenkin, M. E., Derwent, R. G., Hayman, G. D., Alfarra, M. R., Coe, H. and McFiggins, G.:
30 Simulating regional scale secondary organic aerosol formation during the TORCH 2003 campaign in the southern UK, Atmos. Chem. Phys., 6, 419–431, https://doi.org/10.5194/acpd-5-7829-2005, 2006.

Kalberer, M., Sax, M. and Samburova, V.: Molecular size evolution of oligomers in organic aerosols collected in urban atmospheres and generated in a smog chamber, Environ. Sci. Technol., 40(19), 5917–5922, https://doi.org/10.1021/es0525760, 2006.

Knote, C., Hodzic, A., Jimenez, J. L., Volkamer, R., Orlando, J. J., Baidar, S., Brioude, J., Fast, J., Gentner, D. R., Goldstein, A. H., Hayes, P. L., Knighton, W. B., Oetjen, H., Setyan, A., Stark, H., Thalman, R., Tyndall, G., Washenfelder, R., Waxman, E. and Zhang, Q.: Simulation of semi-explicit mechanisms of SOA formation from glyoxal in aerosol in a 3-D model, Atmos. Chem. Phys., 14(12), 6213–6239, https://doi.org/10.5194/acp-14-6213-2014, 2014.

5 Kroll, J. H. and Seinfeld, J. H.: Chemistry of secondary organic aerosol: Formation and evolution of low-volatility organics in the atmosphere, Atmos. Environ., 42(16), 3593–3624, https://doi.org/10.1016/j.atmosenv.2008.01.003, 2008.

Kulmala, M., Laaksonen, A. and Pirjola, L.: Parameterizations for sulfuric acid/water nucleation rates, J. Geophys. Res. Atmos., 103(D7), 8301–8307, https://doi.org/10.1029/97JD03718, 1998.

La, Y. S., Camredon, M., Ziemann, P. J., Valorso, R., Matsunaga, A., Lannuque, V., Lee-Taylor, J., Hodzic, A., Madronich, 10 S. and Aumont, B.: Impact of chamber wall loss of gaseous organic compounds on secondary organic aerosol formation: Explicit modeling of SOA formation from alkane and alkene oxidation, Atmos. Chem. Phys., 16(3), 1417–1431, https://doi.org/10.5194/acp-16-1417-2016, 2016.

Lane, T. E., Donahue, N. M. and Pandis, S. N.: Effect of NOx on secondary organic aerosol concentrations, Environ. Sci. Technol., 42(16), 6022–6027, https://doi.org/10.1021/es703225a, 2008.

15 Lannuque, V., Camredon, M., Couvidat, F., Hodzic, A., Valorso, R., Madronich, S., Bessagnet, B. and Aumont, B.: Exploration of the influence of environmental conditions on secondary organic aerosol formation and organic species properties using explicit simulations: development of the VBS-GECKO parameterization, Atmos. Chem. Phys., 18(18), 13411–13428, https://doi.org/10.5194/acp-18-13411-2018, 2018.

Lemaire, V., Coll, I., Couvidat, F., Mouchel-Vallon, C., Seigneur, C. and Siour, G.: Oligomer formation in the troposphere: 20 From experimental knowledge to 3-D modeling, Geosci. Model Dev., 9(4), 1361–1382, https://doi.org/10.5194/gmd-9-1361-2016, 2016.

Lim, S. S., Vos, T., Flaxman, A. D., Danaei, G., Shibuya, K., Adair-Rohani, H., AlMazroa, M. A., Amann, M., Anderson, H. R., Andrews, K. G., Aryee, M., Atkinson, C., Bacchus, L. J., Bahalim, A. N., Balakrishnan, K., Balmes, J., Barker-Collo, S., Baxter, A., Bell, M. L., Blore, J. D., Blyth, F., Bonner, C., Borges, G., Bourne, R., Boussinesq, M., Brauer, M., Brooks, P., 25 Bruce, N. G., Brunekreef, B., Bryan-Hancock, C., Bucello, C., Buchbinder, R., Bull, F., Burnett, R. T., Byers, T. E., Calabria, B., Carapetis, J., Carnahan, E., Chafe, Z., Charlson, F., Chen, H., Chen, J. S., Cheng, A. T.-A., Child, J. C., Cohen, A., Colson, K. E., Cowie, B. C., Darby, S., Darling, S., Davis, A., Degenhardt, L., Dentener, F., Des Jarlais, D. C., Devries, K., Dherani, M., Ding, E. L., Dorsey, E. R., Driscoll, T., Edmond, K., Ali, S. E., Engell, R. E., Erwin, P. J., Fahimi, S., Falder, G., Farzadfar, F., Ferrari, A., Finucane, M. M., Flaxman, S., Fowkes, F. G. R., Freedman, G., Freeman, M. K., 30 Gakidou, E., Ghosh, S., Giovannucci, E., Gmel, G., Graham, K., Grainger, R., Grant, B., Gunnell, D., Gutierrez, H. R., Hall, W., Hoek, H. W., Hogan, A., Hosgood, H. D., Hoy, D., Hu, H., Hubbell, B. J., Hutchings, S. J., Ibeanusi, S. E., Jacklyn, G. L., Jasrasaria, R., Jonas, J. B., Kan, H., Kanis, J. A., Kassebaum, N., Kawakami, N., Khang, Y.-H., Khatibzadeh, S., Khoo, J.-P., et al.: A comparative risk assessment of burden of disease and injury attributable to 67 risk factors and risk factor

clusters in 21 regions, 1990–2010: a systematic analysis for the Global Burden of Disease Study 2010, Lancet, 380(9859), 2224–2260, https://doi.org/10.1016/S0140-6736(12)61766-8, 2012.

Mailler, S., Menut, L., Khvorostyanov, D., Valari, M., Couvidat, F., Siour, G., Turquety, S., Briant, R., Tuccella, P., Bessagnet, B., Colette, A., Létinois, L., Markakis, K. and Meleux, F.: CHIMERE-2017: From urban to hemispheric

5   chemistry-transport modeling, Geosci. Model Dev., 10(6), 2397–2423, https://doi.org/10.5194/gmd-10-2397-2017, 2017.

Matsunaga, A. and Ziemann, P. J.: Aerosol Science and Technology Gas-Wall Partitioning of Organic Compounds in a Teflon Film Chamber and Potential Effects on Reaction Product and Aerosol Yield Measurements Gas-Wall Partitioning of Organic Compounds in a Teflon Film Chamber and Potential E, Aerosol Sci. Technol., 4410(44), https://doi.org/10.1080/02786826.2010.501044, 2010.

10   McMurry, P. H. and Grosjean, D.: Gas and aerosol wall losses in Teflon film smog chambers, Environ. Sci. Technol., 19(12), 1176–1182, https://doi.org/10.1021/es00142a006, 1985.

Menut, L., Bessagnet, B., Khvorostyanov, D., Beekmann, M., Blond, N., Colette, A., Coll, I., Curci, G., Foret, G., Hodzic, A., Mailler, S., Meleux, F., Monge, J.-L., Pison, I., Siour, G., Turquety, S., Valari, M., Vautard, R. and Vivanco, M. G.: CHIMERE 2013: a model for regional atmospheric composition modelling, Geosci. Model Dev., 6(4), 981–1028,

15   https://doi.org/10.5194/gmd-6-981-2013, 2013.

Ng, N. L., Chhabra, P. S., Chan, a. W. H., Surratt, J. D., Kroll, J. H., Kwan, a. J., McCabe, D. C., Wennberg, P. O., Sorooshian, A., Murphy, S. M., Dalleska, N. F., Flagan, R. C. and Seinfeld, J. H.: Effect of NOx level on secondary organic aerosol (SOA) formation from the photooxidation of terpenes, Atmos. Chem. Phys., 7(4), 5159–5174, https://doi.org/10.5194/acpd-7-10131-2007, 2007.

20   Ntziachristos, L., Gkatzoflias, D., Kouridis, C. and Samaras, Z.: COPERT: A European Road Transport Emission Inventory Model, edited by I. N. Athanasiadis, A. E. Rizzoli, P. A. Mitkas, and J. M. Gómez, pp. 491–504, Springer, Berlin, Heidelberg., 2009.

Odum, J. R., Hoffmann, T., Bowman, F., Collins, D., Flagan, R. C. and Seinfeld, J. H.: Gas particle partitioning and secondary organic aerosol yields, Environ. Sci. Technol., 30(8), 2580–2585, https://doi.org/10.1021/es950943+, 1996.

25   Ots, R., Young, D. E., Vieno, M., Xu, L., Dunmore, R. E., Allan, J. D., Coe, H., Williams, L. R., Herndon, S. C., Ng, N. L., Hamilton, J. F., Bergström, R., Di Marco, C., Nemitz, E., Mackenzie, I. A., Kuenen, J. J. P., Green, D. C., Reis, S. and Heal, M. R.: Simulating secondary organic aerosol from missing diesel-related intermediate-volatility organic compound emissions during the Clean Air for London (ClearfLo) campaign, Atmos. Chem. Phys., 16(10), 6453–6473, https://doi.org/10.5194/acp-16-6453-2016, 2016.

30   Pandis, S. N., Wexler, A. S. and Seinfeld, J. H.: Secondary organic aerosol formation and transport — II. Predicting the ambient secondary organic aerosol size distribution, Atmos. Environ., 27(15), 2403–2416, https://doi.org/10.1016/0960-1686(93)90408-Q, 1993.

Passant, N. R.: Speciation of UK emissions of non-methane volatile organic compounds, AEA Technol. Rep. ENV-0545, (1), 1–289, 2002.

Paulot, F., Crounse, J. D., Kjaergaard, H. G., Kurten, A., St. Clair, J. M., Seinfeld, J. H. and Wennberg, P. O.: Unexpected Epoxide Formation in the Gas-Phase Photooxidation of Isoprene, Science (80-.)., 325(5941), 730–733, https://doi.org/10.1126/science.1172910, 2009.

Petetin, H., Beekmann, M., Sciare, J., Bressi, M., Rosso, A., Sanchez, O. and Ghersi, V.: A novel model evaluation approach focusing on local and advected contributions to urban PM2.5 levels - Application to Paris, France, Geosci. Model Dev., 7(4), 1483–1505, https://doi.org/10.5194/gmd-7-1483-2014, 2014.

Pun, B. K., Griffin, R. J., Seigneur, C. and Seinfeld, J. H.: Secondary organic aerosol 2. Thermodynamic model for gas/particle partitioning of molecular constituents, J. Geophys. Res. Atmos., 107(17), AAC4/1-AAC4/15, https://doi.org/10.1029/2001JD000542, 2002.

Pun, B. K., Wu, S. Y., Seigneur, C., Seinfeld, J. H., Griffin, R. J. and Pandis, S. N.: Uncertainties in modeling secondary organic aerosols: Three-dimensional modeling studies in Nashville/Western Tennessee, Environ. Sci. Technol., 37(16), 3647–3661, https://doi.org/10.1021/es0341541, 2003.

Pun, B. K., Seigneur, C., Vijayaraghavan, K., Wu, S. Y., Chen, S. Y., Knipping, E. M. and Kumar, N.: Modeling regional haze in the BRAVO study using CMAQ-MADRID: 1. Model evaluation, J. Geophys. Res. Atmos., 111(6), 1–25, https://doi.org/10.1029/2004JD005608, 2006a.

Pun, B. K., Seigneur, C. and Lohman, K.: Modeling secondary organic aerosol formation via multiphase partitioning with molecular data, Environ. Sci. Technol., 40(15), 4722–4731, https://doi.org/10.1021/es0522736, 2006b.

Pye, H. O. T., Zuend, A., Fry, J. L., Isaacman-VanWertz, G., Capps, S. L., Appel, K. W., Foroutan, H., Xu, L., Ng, N. L. and Goldstein, A. H.: Coupling of organic and inorganic aerosol systems and the effect on gas&amp;ndash;particle partitioning in the southeastern US, Atmos. Chem. Phys., 18(1), 357–370, https://doi.org/10.5194/acp-18-357-2018, 2018.

Robinson, A. L., Donahue, N. M., Shrivastava, M. K., Weitkamp, E. A., Sage, A. M., Grieshop, A. P., Lane, T. E., Pierce, J. R. and Pandis, S. N.: Rethinking Organic Aerosols: Semivolatile Emissions and Photochemical Aging, Science (80-.)., 315(5816), 1259–1262, https://doi.org/10.1126/science.1133061, 2007.

Rudich, Y., Donahue, N. M. and Mentel, T. F.: Aging of Organic Aerosol: Bridging the Gap Between Laboratory and Field Studies, Annu. Rev. Phys. Chem., 58(1), 321–352, https://doi.org/10.1146/annurev.physchem.58.032806.104432, 2007.

Sarwar, G., Godowitch, J., Henderson, B. H., Fahey, K., Pouliot, G., Hutzell, W. T., Mathur, R., Kang, D., Goliff, W. S. and Stockwell, W. R.: A comparison of atmospheric composition using the Carbon Bond and Regional Atmospheric Chemistry Mechanisms, Atmos. Chem. Phys., 13(19), 9695–9712, https://doi.org/10.5194/acp-13-9695-2013, 2013.

Schauer, J. J., Kleeman, M. J., Cass, G. R. and Simoneit, B. R. T.: Measurement of emissions from air pollution sources. 2. C1 through C30 organic compounds from medium duty diesel trucks, Environ. Sci. Technol., 33(10), 1578–1587, https://doi.org/10.1021/es980081n, 1999.

Schauer, J. J., Kleeman, M. J., Cass, G. R. and Simoneit, B. R. T.: Measurement of emissions from air pollution sources. 5. C1-C32 organic compounds from gasoline-powered motor vehicles., Environ. Sci. Technol., 36(6), 1169–1180, https://doi.org/10.1021/es0108077, 2002.

Schell, B., Ackermann, I. J., Hass, H., Binkowski, F. S. and Ebel, A.: Modeling the formation of secondary organic aerosol within a comprehensive air quality model system, J. Geophys. Res. Atmos., 106(D22), 28275–28293, https://doi.org/10.1029/2001JD000384, 2001.

Schmidt, H., Derognat, C., Vautard, R. and Beekmann, M.: A comparison of simulated and observed ozone mixing ratios for the summer of 1998 in Western Europe, Atmos. Environ., 35(36), 6277–6297, https://doi.org/10.1016/S1352-2310(01)00451-4, 2001.

Shiraiwa, M., Zuend, A., Bertram, A. K. and Seinfeld, J. H.: Gas–particle partitioning of atmospheric aerosols: interplay of physical state, non-ideal mixing and morphology, Phys. Chem. Chem. Phys., 15(27), 11441, https://doi.org/10.1039/c3cp51595h, 2013.

Solazzo, E., Bianconi, R., Pirovano, G., Matthias, V., Vautard, R., Moran, M. D., Wyat Appel, K., Bessagnet, B., Brandt, J., Christensen, J. H., Chemel, C., Coll, I., Ferreira, J., Forkel, R., Francis, X. V, Grell, G., Grossi, P., Hansen, A. B., Miranda, A. I., Nopmongcol, U., Prank, M., Sartelet, K. N., Schaap, M., Silver, J. D., Sokhi, R. S., Vira, J., Werhahn, J., Wolke, R., Yarwood, G., Zhang, J., Rao, S. T. and Galmarini, S.: Operational model evaluation for particulate matter in Europe and North America in the context of AQMEII, Atmos. Environ., 53, 75–92, https://doi.org/10.1016/j.atmosenv.2012.02.045, 2012.

Surratt, J. D., Chan, A. W. H., Eddingsaas, N. C., Chan, M., Loza, C. L., Kwan, A. J., Hersey, S. P., Flagan, R. C., Wennberg, P. O. and Seinfeld, J. H.: Reactive intermediates revealed in secondary organic aerosol formation from isoprene, Proc. Natl. Acad. Sci., 107(15), 6640–6645, https://doi.org/10.1073/pnas.0911114107, 2010.

Tørseth, K., Aas, W., Breivik, K., Fjeraa, A. M., Fiebig, M., Hjellbrekke, A. G., Lund Myhre, C., Solberg, S. and Yttri, K. E.: Introduction to the European Monitoring and Evaluation Programme (EMEP) and observed atmospheric composition change during 1972-2009, Atmos. Chem. Phys., 12(12), 5447–5481, https://doi.org/10.5194/acp-12-5447-2012, 2012.

Trump, E. R. and Donahue, N. M.: Oligomer formation within secondary organic aerosols: equilibrium and dynamic considerations, Atmos. Chem. Phys., 14(7), 3691–3701, https://doi.org/10.5194/acp-14-3691-2014, 2014.

Tsigaridis, K., Daskalakis, N., Kanakidou, M., Adams, P. J., Artaxo, P., Bahadur, R., Balkanski, Y., Bauer, S. E., Bellouin, N., Benedetti, A., Bergman, T., Berntsen, T. K., Beukes, J. P., Bian, H., Carslaw, K. S., Chin, M., Curci, G., Diehl, T., Easter, R. C., Ghan, S. J., Gong, S. L., Hodzic, A., Hoyle, C. R., Iversen, T., Jathar, S., Jimenez, J. L., Kaiser, J. W., Kirkeväg, A., Koch, D., Kokkola, H., H Lee, Y., Lin, G., Liu, X., Luo, G., Ma, X., Mann, G. W., Mihalopoulos, N., Morcrette, J. J., Müller, J. F., Myhre, G., Myriokefalitakis, S., Ng, N. L., O'donnell, D., Penner, J. E., Pozzoli, L., Pringle, K. J., Russell, L. M., Schulz, M., Sciare, J., Seland, Shindell, D. T., Sillman, S., Skeie, R. B., Spracklen, D., Stavrakou, T., Steenrod, S. D., Takemura, T., Tiitta, P., Tilmes, S., Tost, H., Van Noije, T., Van Zyl, P. G., Von Salzen, K., Yu, F., Wang, Z., Wang, Z., Zaveri, R. A., Zhang, H., Zhang, K., Zhang, Q. and Zhang, X.: The AeroCom evaluation and intercomparison of organic aerosol in global models, Atmos. Chem. Phys., 14(19), 10845–10895, https://doi.org/10.5194/acp-14-10845-2014, 2014.

Tsimpidi, a. P., Karydis, V. a., Zavala, M., Lei, W., Molina, L., Ulbrich, I. M., Jimenez, J. L. and Pandis, S. N.: Evaluation of the volatility basis-set approach for the simulation of organic aerosol formation in the Mexico City metropolitan area, Atmos. Chem. Phys., 9(3), 13693–13737, https://doi.org/10.5194/acpd-9-13693-2009, 2010.

Valorso, R., Aumont, B., Camredon, M., Raventos-Duran, T., Mouchel-Vallon, C., Ng, N. L., Seinfeld, J. H., Lee-Taylor, J.

5 and Madronich, S.: Explicit modelling of SOA formation from α-pinene photooxidation: Sensitivity to vapour pressure estimation, Atmos. Chem. Phys., 11(14), 6895–6910, https://doi.org/10.5194/acp-11-6895-2011, 2011.

Vestreng, V.: Review and revision, emission data reported to CLRTAP, , (July), 134 [online] Available from: http://tfeip-secretariat.org/assets/Meetings/Documents/Previous-Meetings/Poland-Sept-2003/ReviewandrevisionMSCWStatusReport2003.pdf, 2003.

10 Volkamer, R., Jimenez, J. L., San Martini, F., Dzepina, K., Zhang, Q., Salcedo, D., Molina, L. T., Worsnop, D. R. and Molina, M. J.: Secondary organic aerosol formation from anthropogenic air pollution: Rapid and higher than expected, Geophys. Res. Lett., 33(17), L17811, https://doi.org/10.1029/2006GL026899, 2006.

Wesely, M. L.: Parameterization of surface resistances to gaseous dry deposition in regional-scale numerical models, Atmos. Environ., 23(6), 1293–1304, https://doi.org/10.1016/0004-6981(89)90153-4, 1989.

15 WHO Regional Office for Europe OECD: Economic cost of the health impact of air pollution in Europe: Clean air, health and wealth., Eur. Environ. Heal. Process., 1–54, 2015.

Woody, M. C., West, J. J., Jathar, S. H., Robinson, A. L. and Arunachalam, S.: Estimates of non-traditional secondary organic aerosols from aircraft SVOC and IVOC emissions using CMAQ, Atmos. Chem. Phys., 15(12), 6929–6942, https://doi.org/10.5194/acp-15-6929-2015, 2015.

20 Zhao, Y., Nguyen, N. T., Presto, A. A., Hennigan, C. J., May, A. A. and Robinson, A. L.: Intermediate Volatility Organic Compound Emissions from On-Road Diesel Vehicles: Chemical Composition, Emission Factors, and Estimated Secondary Organic Aerosol Production, Environ. Sci. Technol., 49(19), 11516–11526, https://doi.org/10.1021/acs.est.5b02841, 2015.

Zhao, Y., Nguyen, N. T., Presto, A. A., Hennigan, C. J., May, A. A. and Robinson, A. L.: Intermediate Volatility Organic Compound Emissions from On-Road Gasoline Vehicles and Small Off-Road Gasoline Engines, Environ. Sci. Technol.,

25 50(8), 4554–4563, https://doi.org/10.1021/acs.est.5b06247, 2016.

Zhu, S., Sartelet, K. N., Healy, R. M. and Wenger, J. C.: Simulation of particle diversity and mixing state over Greater Paris: a model–measurement inter-comparison, Faraday Discuss., 189(189), 547–566, https://doi.org/10.1039/C5FD00175G, 2016a.

Zhu, S., Sartelet, K., Zhang, Y. and Nenes, A.: Three-dimensional modeling of the mixing state of particles over Greater

30 Paris, J. Geophys. Res. Atmos., 121(10), 5930–5947, https://doi.org/10.1002/2015JD024241, 2016b.

Atmospheric
Chemistry
and Physics
Discussions

Table 1 – List of the VBS-GECKO species and associated properties.

Species	Partition[b]	MW (g.mol^{-1})	P^{sat}_{298K} (atm)	H^{eff}_{298K} (mol.L^{-1}.atm^{-1})	ΔH_{vap} (kJ.mol^{-1})
α-pinene		136	4.47×10^{-3}	1.70×10^{-2}	46
β-pinene		136	4.79×10^{-3}	1.70×10^{-2}	45
Limonene		136	4.57×10^{-3}	1.70×10^{-2}	46
Benzene		78	6.61×10^{-2}	0.21	36
Toluene		92	2.14×10^{-2}	0.18	40
O-xylene		106	7.24×10^{-3}	0.25	45
M-xylene		106	5.75×10^{-3}	0.16	45
P-xylene		106	7.24×10^{-3}	0.17	45
decane		142	1.90×10^{-3}	1.41×10^{-4}	50
Tetradecane	*	198	3.63×10^{-5}	7.94×10^{-5}	66
Octadecane	*	254	7.76×10^{-7}	2.57×10^{-5}	83
Docosane	*	310	1.66×10^{-8}	8.51×10^{-6}	100
Hexacosane	*	366	3.39×10^{-10}	2.82×10^{-6}	118
Decene		140	2.04×10^{-3}	1.00×10^{-3}	50
Tetradecene	*	196	3.98×10^{-5}	3.31×10^{-4}	66
Octadecene	*	253	8.71×10^{-7}	1.10×10^{-4}	82
Docosene	*	308	1.91×10^{-8}	3.63×10^{-5}	99
Hexacosene	*	364	4.07×10^{-10}	1.20×10^{-5}	117
VB1[a]	*	210	3.16×10^{-7}	1.0×10^{6}	90
VB2[a]	*	240	1.0×10^{-8}	1.0×10^{7}	105
VB3[a]	*	270	1.0×10^{-9}	1.0×10^{8}	115
VB4[a]	*	300	1.0×10^{-10}	1.0×10^{9}	125
VB5[a]	*	330	1.0×10^{-11}	1.0×10^{10}	135
VB6[a]	*	360	1.0×10^{-12}	1.0×10^{11}	145
VB7[a]	*	390	1.0×10^{-14}	1.0×10^{12}	165

[a] Properties of the bins do not depend on the precursor (see Lannuque et al., 2018)
[b] Gas/particle partitioning is implemented in CHIMERE for species with a * only

5 **Table 2 – Distribution of the NMVOC emission in the VBS-GECKO species.**

VBS-GECKO	Emitted NMVOC in CHIMERE (Passant, 2002)
Decane	C10 alkanes; C10 cycloalkanes; 75% of C11 alkanes; 50% of C12 alkanes; 25% of C13 alkanes
Tetradecane	25% of C11 alkanes; 50% of C12 alkanes; 75% of C13 alkanes
Decene	C10 alkenes
Benzene	Benzene
Toluene	25% of C9, C10, C13 and unspeciated aromatic hydrocarbons, ethylbenzene, isopropylbenzene, propylbenzene, phenol, toluene and styrene
O-xylene	25% of C9, C10, C13 and unspeciated aromatic hydrocarbons; 2-ethyltoluene; indan; 33% of ethyltoluene; 33% of methylpropylbenzene; o-xylene
M-xylene	25% of C9, C10, C13 and unspeciated aromatic hydrocarbons, tetramethylbenzene; trimethylbenzene; 1-methyl-3-isopropylbenzene; 3-ethyltoluene; ethyldimethylbenzene; 33% of ethyltoluene; 33% of methylpropylbenzene; m-xylene
P-xylene	25% of C9, C10, C13 and unspeciated aromatic hydrocarbons; 1-methyl-4-isopropylbenzene; 4-ethyltoluene; 33% of ethyltoluene; 33% of methylpropylbenzene; p-xylene

Atmospheric
Chemistry
and Physics
Discussions

Table 3 – Statistical results calculated on daily averaged concentrations for the ref-VBS-GECKO simulations and differences between ref-VBS-GECKO and H^{2}O statistical indicators.

	Observations		VBS-GECKO results					Differences with H^{2}O results				
	Number	Mean	Mean	RMSE	R	MFB	MFE	Δ mean	Δ RMSE	Δ R	Δ MFB	Δ MFE
	-	(µg.m^{-3})	(µg.m^{-3})	(µg.m^{-3})	-	-	-	(%)	(%)	-	(dist from 0)	-
PM$_{2.5}$	2002	9.07	7.65	6.14	0.42	-0.09	0.37	+5.52	-1.76	+0.01	-0.05	-0.01
OM$_{PM1}$	237	3.24	1.93	2.28	0.79	-0.47	0.57	+31.3	-11.6	-0.04	-0.25	-0.17
OC$_{PM2.5}$	235	2.52	2.59	1.75	0.57	-0.16	0.51	+15.6	+5.42	+0.02	-0.17	-0.08

5

Table 4 – Statistical results calculated on daily averaged concentrations simulated with the various model configurations and differences with the ref-VBS-GECKO configuration statistical indicators given Table 3.

		Sensitivity test results					Differences to ref-VBS-GECKO results				
		Mean	RMSE	R	MFB	MFE	Δ mean	Δ RMSE	Δ R	Δ MFB	Δ MFE
Model configuration		(µg.m^{-3})	(µg.m^{-3})	-	-	-	(%)	(%)	-	(dist from 0)	-
hydro-VBS-GECKO	OM$_{PM1}$	1.93	2.28	0.79	-0.47	0.57	0.00	0.00	0.00	0.00	0.00
	OC$_{PM2.5}$	2.59	1.75	0.57	-0.16	0.51	0.00	0.00	0.00	0.00	0.00
hydro-VBS-GECKO-high	OM$_{PM1}$	2.07	2.17	0.79	-0.41	0.52	+7.43	-4.58	0.00	-0.06	-0.05
	OC$_{PM2.5}$	2.71	1.73	0.57	-0.11	0.48	+4.80	-0.65	0.00	-0.05	-0.03
k$_{OH}$-VBS-GECKO-low	OM$_{PM1}$	1.87	2.32	0.78	-0.49	0.59	-2.70	+1.90	-0.01	+0.02	+0.02
	OC$_{PM2.5}$	2.52	1.73	0.57	-0.19	0.53	-2.40	-0.65	0.00	+0.03	+0.02
k$_{OH}$-VB-GECKO-high	OM$_{PM1}$	2.02	2.21	0.79	-0.43	0.54	+4.72	-2.67	0.00	-0.04	-0.03
	OC$_{PM2.5}$	2.70	1.76	0.57	-0.12	0.49	+4.32	+0.65	0.00	-0.04	-0.02
RRR-VBS-GECKO-low	OM$_{PM1}$	2.11	2.13	0.80	-0.41	0.52	+9.45	-6.48	0.01	-0.06	-0.05
	OC$_{PM2.5}$	2.82	1.81	0.57	-0.08	0.48	+9.13	+3.92	0.00	-0.08	-0.03
RRR-VBS-GECKO-high	OM$_{PM1}$	1.73	2.42	0.78	-0.54	0.64	-10.1	+6.48	-0.01	+0.07	+0.07
	OC$_{PM2.5}$	2.36	1.72	0.56	-0.25	0.56	-8.65	-1.30	-0.01	+0.09	+0.05
P^{sat}-VBS-GECKO-low	OM$_{PM1}$	2.42	1.92	0.80	-0.31	0.44	+25.6	-15.6	+0.01	-0.16	-0.13
	OC$_{PM2.5}$	3.17	1.99	0.58	0.02	0.45	+22.5	+13.7	+0.01	-0.18	-0.06
P^{sat}-VBS-GECKO-high	OM$_{PM1}$	1.47	2.63	0.76	-0.65	0.73	-23.6	+15.6	-0.03	+0.18	+0.16
	OC$_{PM2.5}$	2.07	1.76	0.56	-0.36	0.63	-19.7	+0.65	-0.01	+0.20	+0.12

10

Atmospheric
Chemistry
and Physics
Discussions

Table 5 – Distribution of the VBS-GECKO surrogate species for IVOC emission in the various model configurations.

Model configuration	Species			
	C14	C18	C22	C26
150 % POA	105 % of POA	80 % POA	40 % of POA	25 % of POA
4 % VOC	2.8 % of NMVOC	35 % of POA + 1,2 % of NMVOC	40 % of POA	25 % of POA
16 % VOC	11.2 % of NMVOC	35 % of POA + 4.8 % of NMVOC	40 % of POA	25 % of POA
30 % VOC	21 % of NMVOC	35 % of POA + 9 % of NMVOC	40 % of POA	25 % of POA
65 % VOC	45.5 % of NMVOC	35 % of POA + 19.5 % of NMVOC	40 % of POA	25 % of POA

Table 6 – Statistical results calculated on daily averaged concentrations simulated with VBS-GECKO considering IVOC emissions
5 **and differences with those of the ref-VBS-GECKO (without IVOC) from Table 3.**

Model configuration		VBS-GECKO with IVOC results					Differences with ref-VBS-GECKO				
		Mean	RMSE	R	MFB	MFE	Δ Mean	Δ RMSE	Δ R	Δ MFB	Δ MFE
		($\mu g.m^{-3}$)	($\mu g.m^{-3}$)	-	-	-	%	%	-	(dist from 0)	-
IVOC$_{150POA}$	**OM$_{PM1}$**	2.02	2.18	0.80	-0.43	0.53	+4.66	-4.38	+0.01	-0.04	-0.04
	OC$_{PM2.5}$	2.72	1.83	0.57	-0.11	0.5	+5.01	+4.57	0.00	-0.05	-0.01
IVOC$_{4VOC}$	**OM$_{PM1}$**	1.96	2.24	0.79	-0.46	0.56	+1.55	-1.75	0.00	-0.01	-0.01
	OC$_{PM2.5}$	2.64	1.79	0.57	-0.15	0.51	+1.93	+2.28	0.00	-0.01	0.00
IVOC$_{16VOC}$	**OM$_{PM1}$**	2.01	2.20	0.8	-0.44	0.54	+4.14	-3.50	+0.01	-0.03	-0.03
	OC$_{PM2.5}$	2.73	1.88	0.57	-0.12	0.51	+5.40	+7.42	0.00	-0.04	0.00
IVOC$_{30VOC}$	**OM$_{PM1}$**	2.06	2.15	0.80	-0.42	0.53	+6.73	-5.70	+0.01	-0.05	-0.04
	OC$_{PM2.5}$	2.84	1.98	0.57	-0.09	0.51	+9.65	+13.1	0.00	-0.07	0.00
IVOC$_{65VOC}$	**OM$_{PM1}$**	2.18	2.04	0.81	-0.37	0.50	+12.9	-10.5	+0.02	-0.10	-0.07
	OC$_{PM2.5}$	3.10	2.29	0.56	-0.02	0.50	+19.6	+30.8	-0.01	-0.14	-0.01
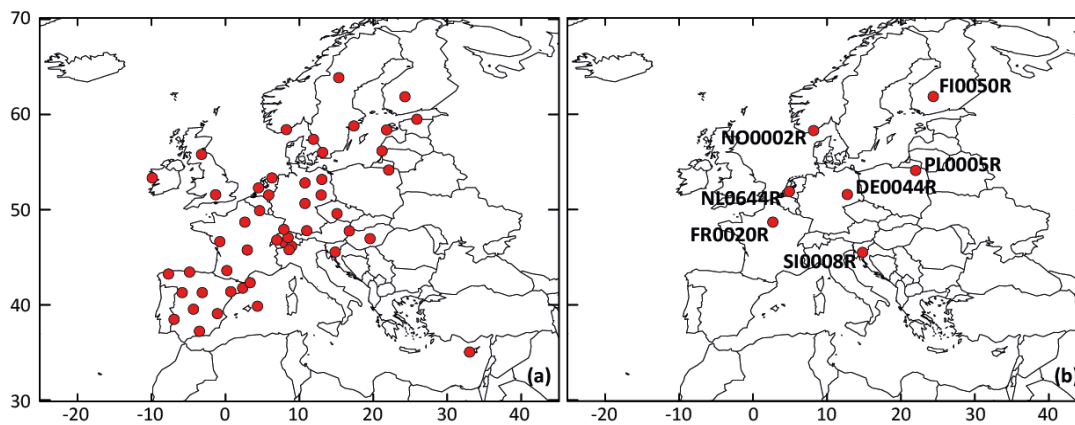
Figure 1 – Location of rural background stations used for (a) the statistical evaluations and (b) time series comparisons.
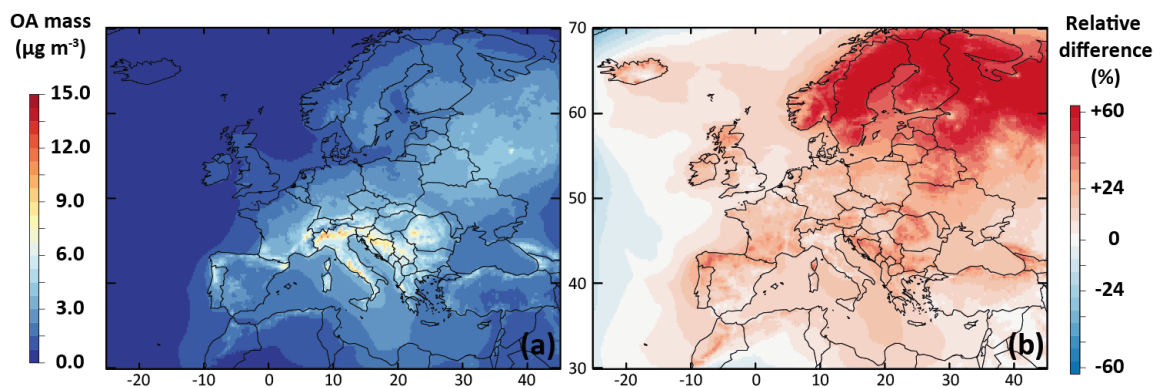
5

10

Figure 2 – Mean OA mass concentrations simulated with the ref-VBS-GECKO model configuration over Europe for the July-August 2013 period (a) and relative difference of the simulated mean OA mass concentrations between the ref-VBS-GECKO and the H^2O configuration (b).
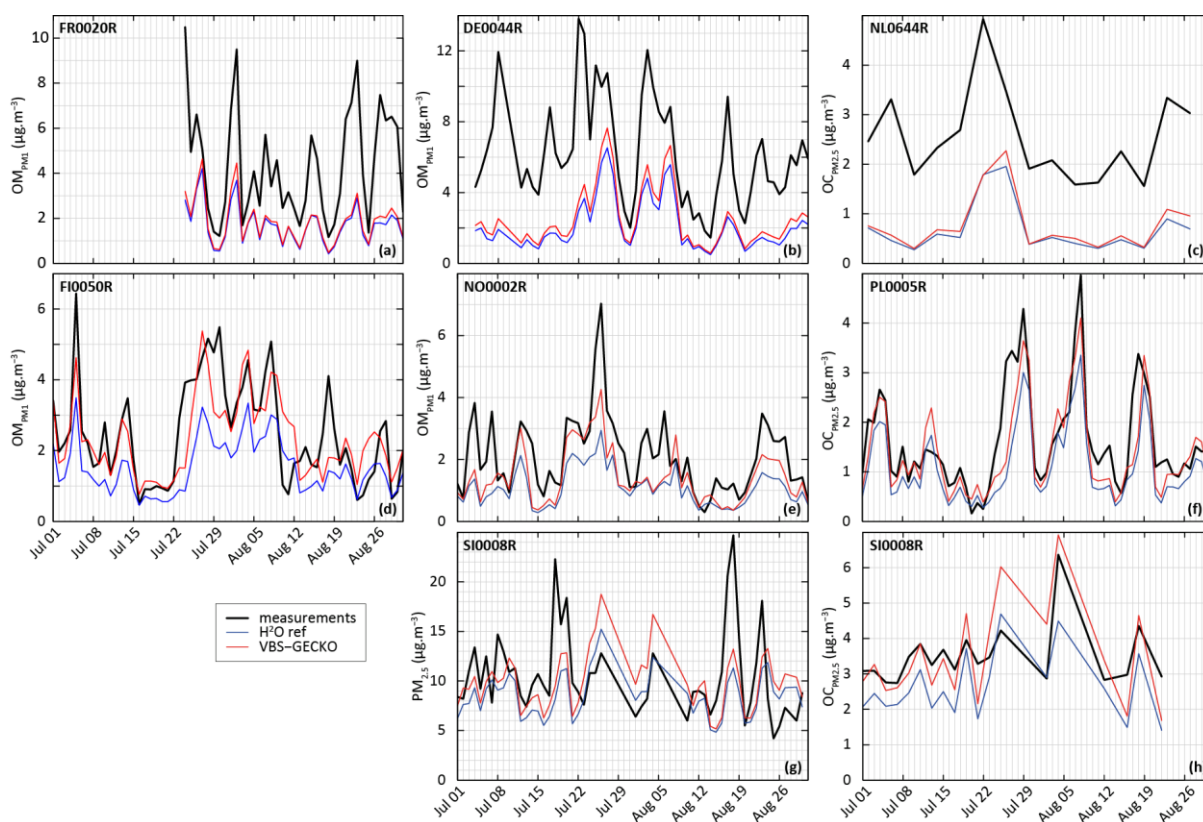

Figure 3 – Measured (black) and simulated (with H^2O in blue and ref-VBS-GECKO in red) temporal evolution of daily averaged OM_{PM1} concentrations (panels a, b, d and e) $OC_{PM2.5}$ concentrations (panels c, f and h) and $PM_{2.5}$ concentrations (panel g). Top panels are for stations influenced by anthropogenic sources in France (FR0020R station, a), Germany (DE0044R station, b) and Netherland (NL0644R station, c), middle panels are stations in remote areas in Finland (FIOO50R station, d), Norway (NO0002R station, d) and Poland (PL0005R station, e) and bottom panels are for a station located in a remote area in Slovenia (g and h).
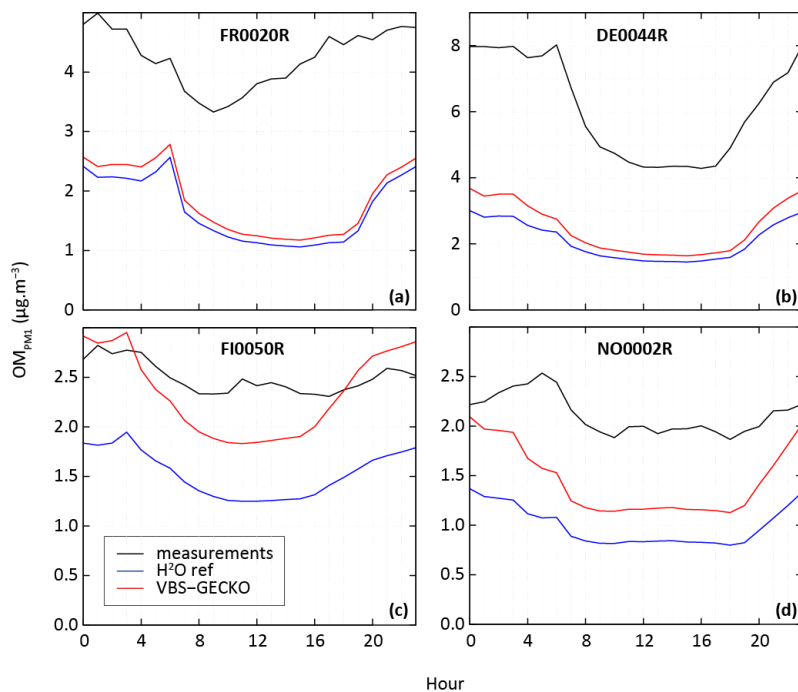
Figure 4 – Measured (black) and simulated mean diurnal profile (in UTC) with the H^2O model configuration (blue) and the ref-VBS-GECKO model configuration (red) for OM_{PM1} concentration at stations influenced dominantly by anthropogenic sources (FR0020R (a) and DE0044R (b)) and by biogenic sources (FI0050R (c) and NO0002R (d)).
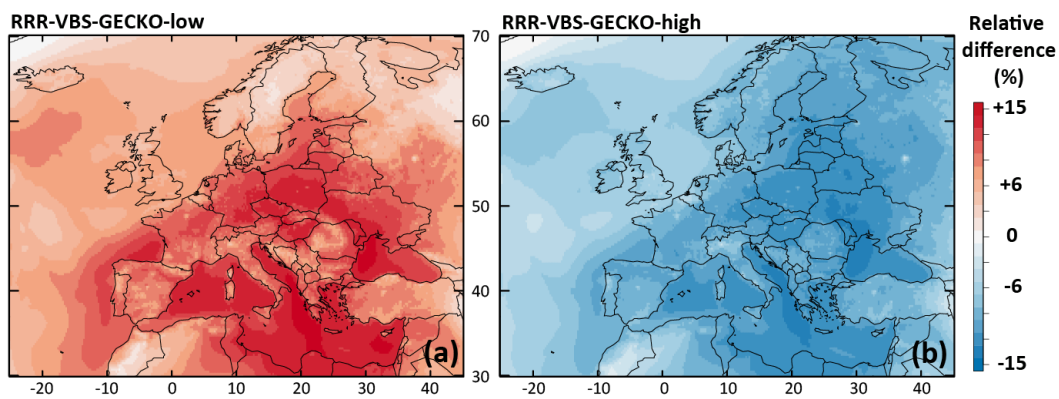
5
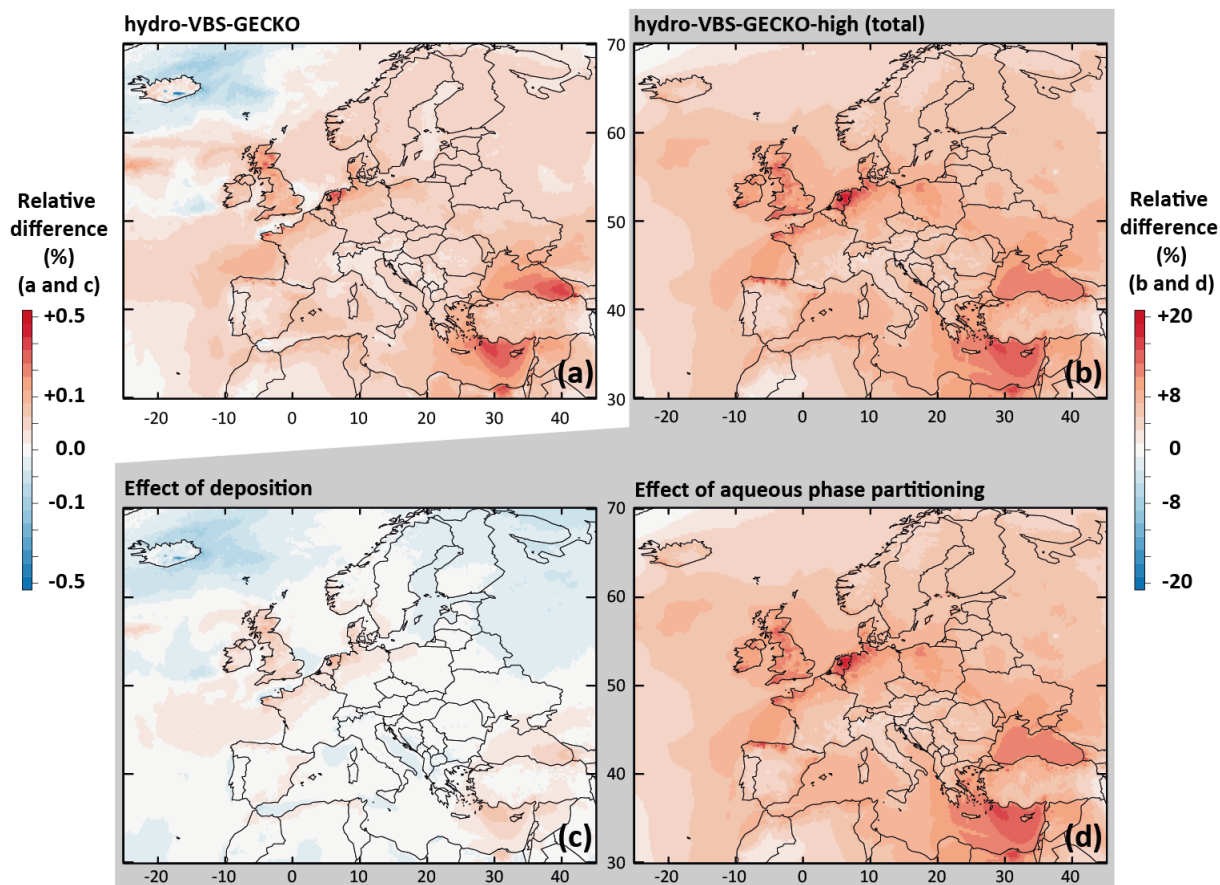
Figure 5 – Relative differences on the simulated mean OA concentrations between (a) the Hydro-VBS-GECKO and the ref-VBS-GECKO and (b) the Hydro-VBS-GECKO-high and the ref-VBS-GECKO model configurations for the two-month period. Bottom panels represent relative differences on the simulated mean OA concentrations between the Hydro-VBS-GECKO-high and the ref-VBS-GECKO due to variation in deposition (c) or partitioning (d).
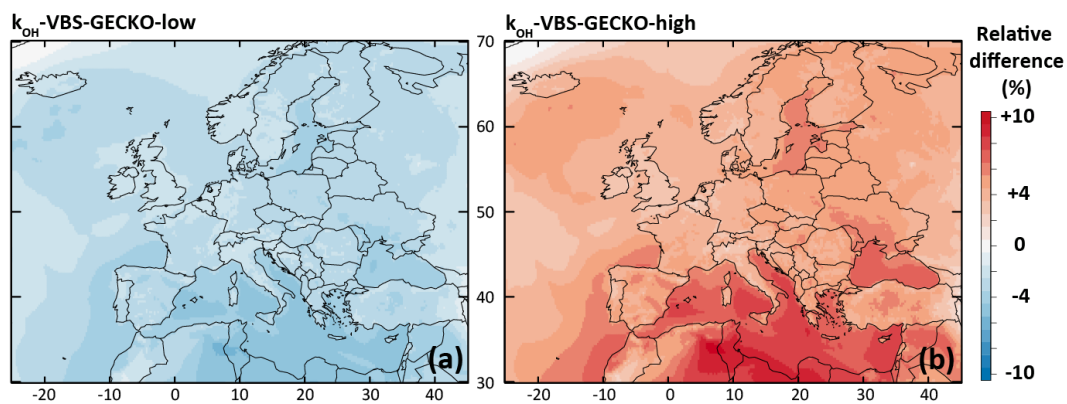
Figure 6 – Relative differences on the simulated mean OA concentrations between (a) the k_{OH}-VBS-GECKO-low and the ref-VBS-GECKO model configurations and (b) the k_{OH}-VBS-GECKO-high and the ref-VBS-GECKO model configurations for the two-month period.

Atmospheric
Chemistry
and Physics
Discussions
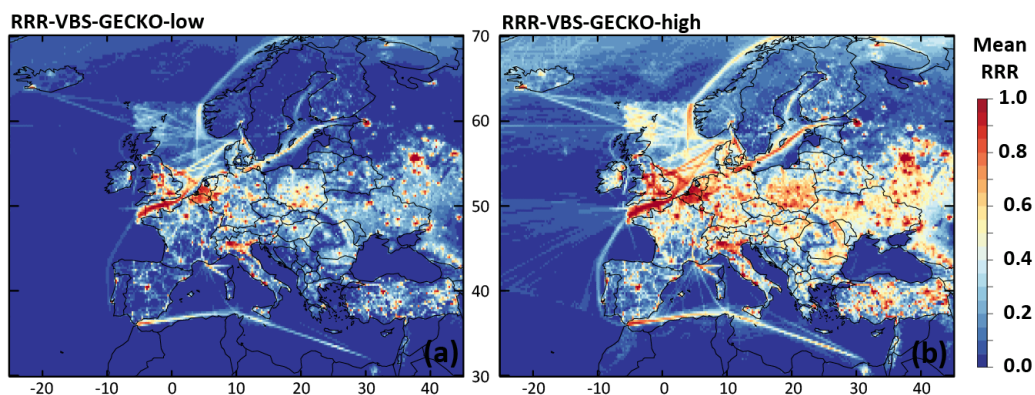
Figure 7 – Mean RRR over Europe during the two-month period for (a) the RRR-VBS-GECKO-low and (b) the RRR-VBS-GECKO-high model configurations.

Figure 8 – Relative differences on the simulated mean OA concentrations between (a) the RRR-VBS-GECKO-low and the ref-VBS-GECKO model configurations and (b) between the RRR-VBS-GECKO-high and the ref-VBS-GECKO model configurations for the two-month period.

Atmospheric
Chemistry
and Physics
Discussions
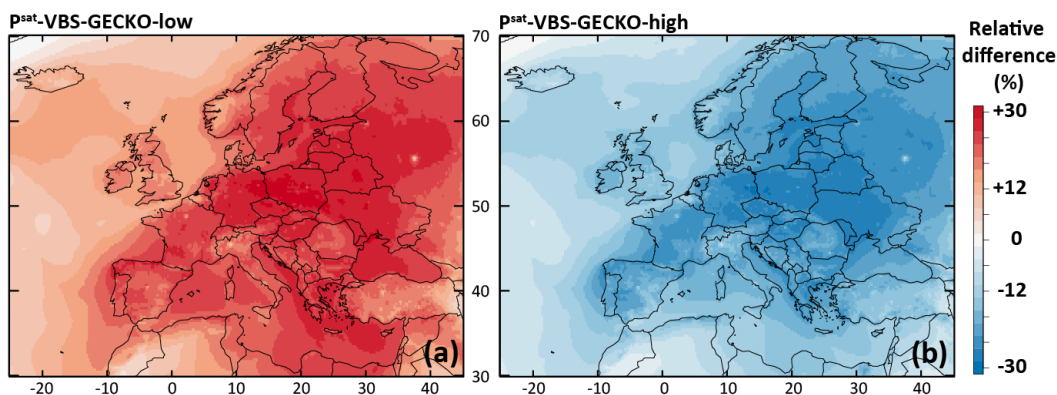
Figure 9 – Relative difference on the simulated mean OA concentrations between (a) the P^{sat}-VBS- -low and the ref-VBS-GECKO model configurations and (b) between the P^{sat}-VBS-GECKO-high and the ref-VBS-GECKO model configurations for the two-month period.

5
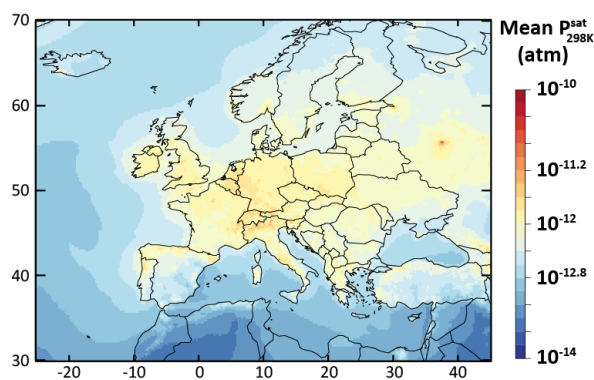
Figure 10 – Simulated average volatility of OA in term of P^{sat}_{298K} upon Europe during the July-August 2013 period for the ref-VBS-GECKO model configuration.
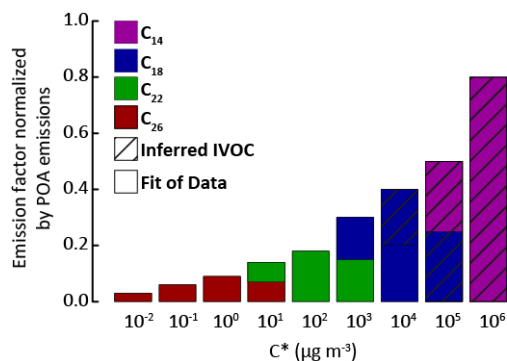
10 **Figure 11 – Distribution of the VBS-GECKO species into the SVOC and IVOC volatility bins of Robinson et al. (2007). Normalized emission factors by POA emissions for IVOC are used for the $IVOC_{150POA}$ model configuration.**
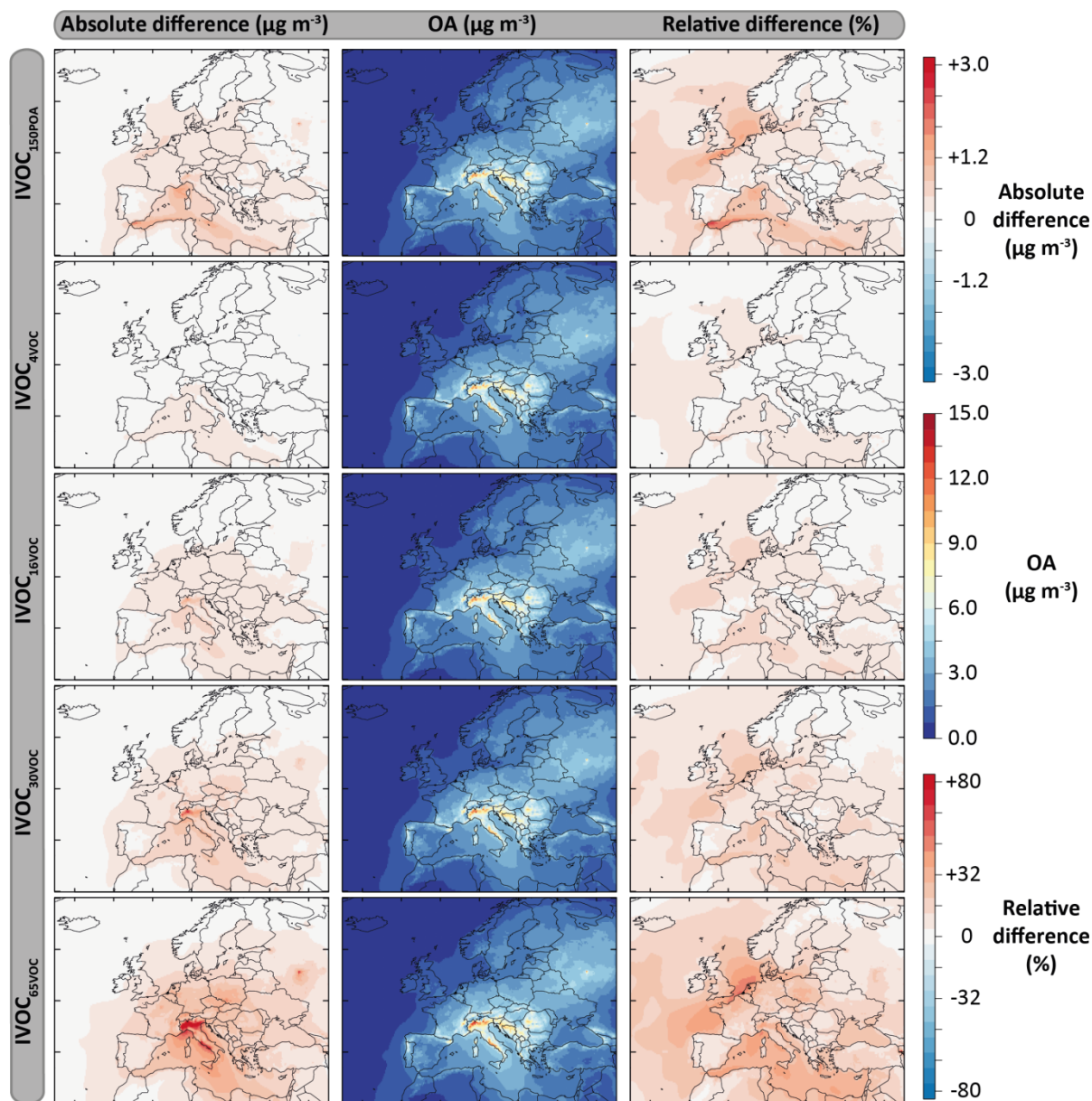
Figure 12 – Mean OA mass concentrations simulated with the model configurations including the IVOC emissions for the July-August 2013 period over Europe (second column), and absolute and relative differences with the ref-VBS-GECKO model configurations (left and right columns respectively). Results are given for the following model configurations: IVOC$_{150POA}$ (first row), IVOC$_{4VOC}$ (second ro), IVOC$_{16VOC}$ (third row), IVOC$_{30VOC}$ (fourth row) and IVOC$_{65VOC}$ (fifth row).
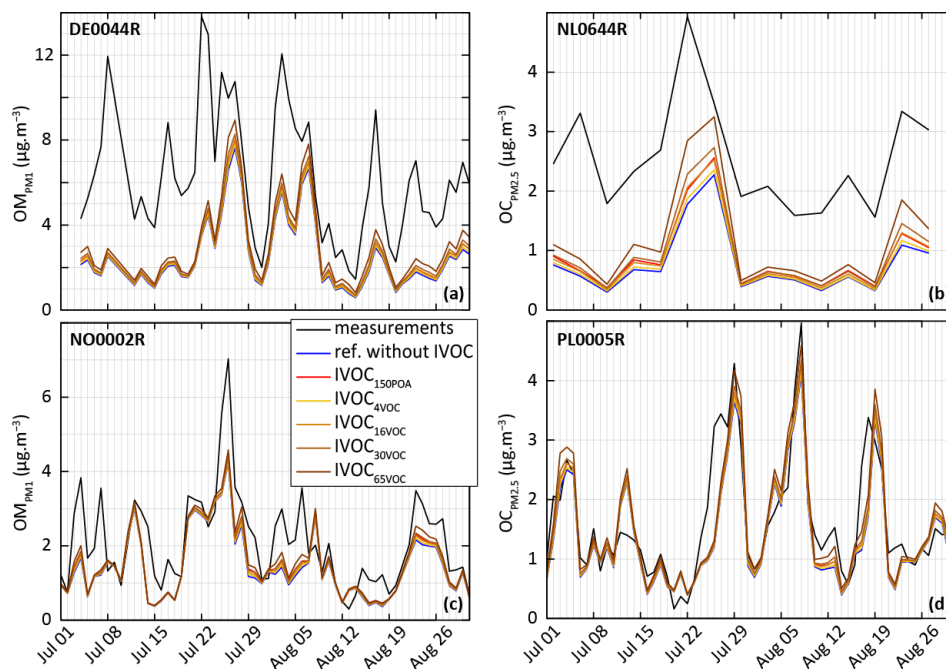
Figure 13 – Measured and simulated (for the ref-VBS-GECKO configuration without IVOC and the different model configuration considering IVOC emissions) temporal evolution of daily averaged OM$_{PM1}$ concentrations (panels a and c) and OC$_{PM2.5}$ concentrations (panels b and d). Top panels are for stations close to anthropogenic sources in Germany (DE0044R station, a) and Netherland (NL0644R station, b) and bottom panels for stations in remote areas in Norway (NO0002R station, c) and Poland (PL0005R station, d).
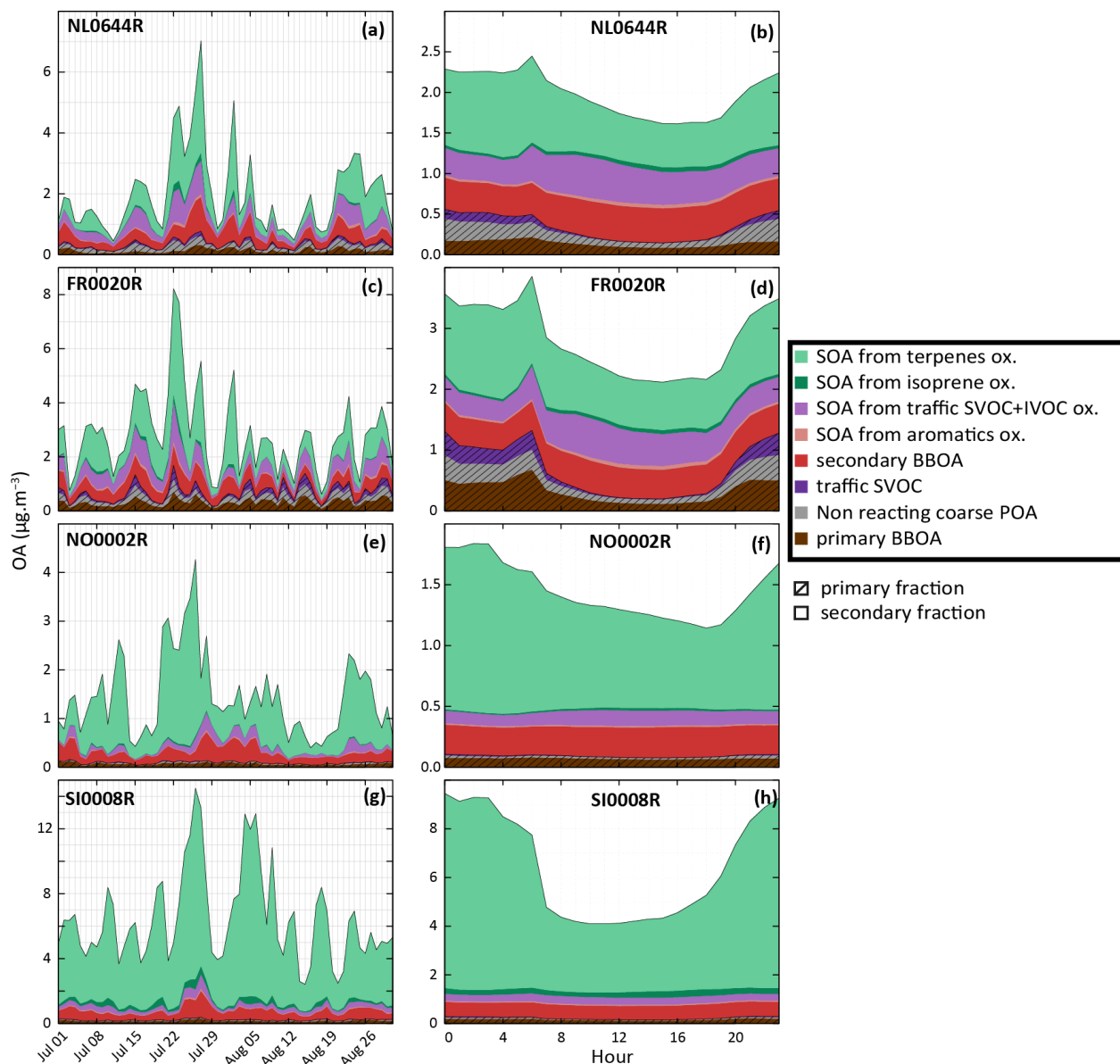
Figure 14 – Evolution of simulated OA concentrations and distribution function of sources with the IVOC$_{30VOC}$ model configuration. Panels a, c, e and g present evolutions of daily average concentrations during the July-August 2013. Panels b, d, f and h present mean daily profiles. Results are shown at two stations influenced by anthropogenic sources in Netherland (NL0644R, a and b) and in France (FR0020R, c and d) and at two stations influenced by biogenic sources in Norway (NL0002R, e and f) and Slovenia (SI0008R, g and h). Primary and secondary BBOA includes compounds from biomass burning. Traffic SVOC includes C$_{14}$ to C$_{26}$ VBS-GECKO alkanes and alkenes and SOA from traffic SVOC+IVOC includes their oxidation products. SOA from terpenes includes all species produced by α-pinene, β-pinene, limonene, ocimene and humulene oxidation.
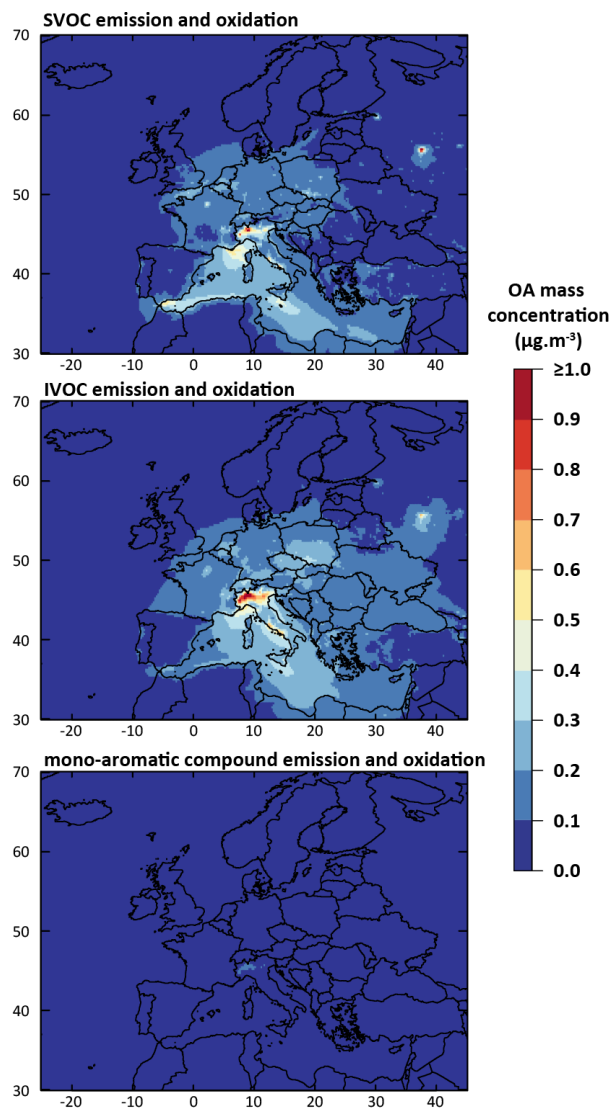
Figure 15 – Mean simulated anthropogenic OA mass concentration formed by the partitioning of species produced from the oxidation of emitted SVOC (a), IVOC (b) and mono-aromatic compound (c) for July-August 2013 over Europe (data from IVOC$_{30VOC}$ simulation).

5